Hum-Power Controller for Powered Wheelchairs

A thesis submitted in partial fulfillment of the requirements for the degree of Master of Science at George Mason University

By

Hossein Ghaffari Nik
Bachelor of Science
George Mason University, 2007

Director: Dr. Nathalia Peixoto, Assistant Professor
Department of Electrical and Computer Engineering

Summer Semester 2009
George Mason University
Fairfax, VA

Copyright: 2009 Hossein Ghaffari Nik
All Rights Reserved

DEDICATION

This is dedicated to my family for their never-ending love and support. To my parents, Kazem Ghaffari Nik and Parivash Godazgari without whom I wouldn’t be standing where I am today and to my dearest sister Sara Ghaffari Nik for her love and support.

ACKNOWLEDGEMENTS

I would like to thank my advisor Dr. Nathalia Peixoto for her guidance, encouragements and support throughout this project. I would also like to thank East Coast Rehab LLC for their donation to this project and providing us with a powered wheelchair for development and testing.

TABLE OF CONTENTS

Page

LIST OF TABLES vi

LIST OF FIGURES vii

ABSTRACT ix

CHAPTER 1: INTRODUCTION 1

- 1.1. PROBLEM STATEMENT 1
- 1.2. COMMERCIALLY AVAILABLE SOLUTIONS 2
- 1.3. PROPOSED SOLUTIONS 6

CHAPTER 2: PROTOTYPE DEVELOPMENT 13

- 2.1. MATLAB ENVIRONMENT 13
  - i. GMU Neurot 13
- 2.2. LABVIEW ENVIRONMENT 22
  - i. Voice Activated RC Car 22
  - ii. Voice Activated Mini Lego Chair 24

CHAPTER 3: MICROCONTROLLER IMPLEMENTATION FOR WHEELCHAIR 25

- 3.1. EVALUATION BOARD 25
- 3.2. dsPIC30F MICROCONTROLLER 28
- 3.3. DESIGNED BOARD 32
  - i. Speech Recognition Engine 32
  - ii. Humming Detection Technique 36
  - iii. Powered Wheelchair Interface 43
- 3.4. AMBIENT NOISE TEST RESULTS 49
- 3.5. FIELD TEST RESULTS 57

CHAPTER 4: DISCUSSION 58

- 4.1. WHAT WAS ACHIEVED IN THIS THESIS 58
- 4.2. FUTURE WORK 60

APPENDIX 62

OPERATION MANUAL 62

REFERENCES 68

LIST OF TABLES

Table Page

TABLE 1. BREAK DOWN OF POWER WHEELCHAIR CONTROL INTERFACES USED IN AVERAGE 3

TABLE 2. ADEQUACY OF EXISTING CONTROL INTERFACES 4

TABLE 3. PROPORTION OF PATIENTS UNABLE TO USE A POWER WHEELCHAIR 5

TABLE 4. COMPLETE LIST OF VOICE COMMANDS FOR HUM-POWER CONTROLLER INTERFACE 10

TABLE 5. ACCURACY OF MFCC BASED SPEECH RECOGNITION FOR GMU NEUROT 22

LIST OF FIGURES

Figure Page

FIGURE 1. COMMON COMMERCIALLY AVAILABLE CONTROLLERS FOR POWERED WHEELCHAIRS 3

FIGURE 2. SYSTEMATIC DIAGRAM OF HUM-POWER CONTROLLER FOR POWERED WHEELCHAIRS 8

FIGURE 3. SYSTEM FLOW OF THE HUM-POWER CONTROLLER FOR POWERED WHEELCHAIRS 9

FIGURE 4. GMU NEUROT: THE VOICE ACTIVATED ROBOTIC ARM 14

FIGURE 5. SPEECH RECOGNITION PROCESS BASED ON MFCC FOR GMU NEUROT 15

FIGURE 6. GMU NEUROT'S CONTROL PANEL COMPUTER INTERFACE 16

FIGURE 7. MFCC REPRESENTATION OF VOICE SIGNAL 17

FIGURE 8. CROSS CORRELATION RESULTS FOR THE MFCC'S OF DIFFERENT WORDS. 21

FIGURE 9. VOICE ACTIVATED RC CAR USING LABVIEW 23

FIGURE 10. VOICE ACTIVATED MINI LEGO CHAIR USING LABVIEW 24

FIGURE 11. THE DSPICDEM™ PLUS DEVELOPMENT BOARD WITH MPLAB ICD 2.... 26

FIGURE 12. DSPIC30F6014A PLUG-IN MODULE 27

FIGURE 13. THE DSPIC30F6014A BLOCK DIAGRAM 30

FIGURE 14. OVERVIEW OF SPEECH RECOGNITION 33

FIGURE 15. OVERVIEW OF SPEECH RECOGNITION FLOW DIAGRAM 35

FIGURE 16. HUM DETECTION BOARD 37

FIGURE 17. FAST FOURIER TRANSFORM 38

FIGURE 18. THE FFT DECOMPOSITION 39

FIGURE 19. THE FFT BIT REVERSAL SORTING 40

FIGURE 20. FLOW DIAGRAM OF THE FFT 42

FIGURE 21. HUM-POWER CONTROLLER BOARD 45

FIGURE 22. BLOCK DIAGRAM OF THE HUM-POWER CONTROLLER 46

FIGURE 23. SCHEMATICS OF DSPIC FOR SPEECH RECOGNITION 47

FIGURE 24. SCHEMATICS OF DSPIC PERFORMING FFT 48

FIGURE 25. SCHEMATICS OF SI3000 CODEC 49

FIGURE 26. MEASURED SIGNAL POWER WITHOUT ADDED NOISE 50

FIGURE 27. MEASURED SIGNAL POWER FOR DIFFERENT WHITE GAUSSIAN NOISE LEVELS 51

FIGURE 28. CALCULATED NOISE POWER FROM THE MEASURED NOISY SIGNAL 52

FIGURE 29. CALCULATED SIGNAL-TO-NOISE RATIO OF THE MEASURED NOISY SIGNAL AT DIFFERENT VOLUE LEVELS 53

FIGURE 30. POWER PROFILE FOR THE NOISE SOURCE WITH DIFFERENT INTENSITY LEVELS 54
FIGURE 31. RELIABILITY PROFILE OF SIGNAL POWER MEASUREMENT FOR THE SPOKEN WORDS 55
FIGURE 32. SPEECH RECOGNITION ACCURACY AT DIFFERENT SNR LEVELS 56
FIGURE 33. HUM-POWER CONTROLLER INSTALLED ON POWERED WHEELCHAIR 59

ABSTRACT

HUM-POWER CONTROLLER FOR POWERED WHEELCHAIRS

Hossein Ghaffari Nik, MS

George Mason University, 2009

Thesis Director: Dr. Nathalia Peixoto

The objective of this work is to create a control mechanism for smooth operation of powered wheelchairs through speech recognition and humming detection. Users of wheelchairs are estimated to be about 200 million people worldwide. In the U.S.A., roughly 11000 people are affected by spinal cord injury every year, with 47 percent of those accidents leading to quadriplegia [15]. The technology developed in the last ten years for assistive technology will significantly impact and improve the life of wheelchair users. While current powered wheelchairs, originally designed to facilitate maneuvering through indoor and outdoor areas, have helped millions of people with their handicap, many of these users state that power chairs do not entirely fulfill their needs. A survey of currently commercialized control systems for powered wheelchairs resulted in identification of many shortcomings [15, 30]. Joysticks, head-arrays and push-button controllers all require precise and accurate movement in the hands or neck for smooth operation of the power chair. Sip-n-puff controllers solve the latter issue, where the user

is able to control the movement of the chair using specific suck and blow operations on a tube. Although this controller solves the mobility problem of the users, it is still awkward and unpleasant to use in public [2, 9, 10].

The main shortcoming we detected was the lack of smooth control in speed and direction of movement due to patients' physical limitations. To resolve this deficiency we designed, developed, and tested a new control unit that interfaces with commercially available wheelchairs. Our controller utilizes speech recognition technology and facilitates hands free operation of power chairs by all users through simple voice commands. Digital signal processing is also implemented to tackle smooth control limitations. The Hum-power controller allows the user to smoothly change the speed of the chair using the frequency of their humming which is captured via an accelerometer attached to their neck. This controller enables complete hands free smooth control of the powered wheelchairs for all users and especially for those who cannot use conventional controllers.

We currently use two digital signal processors from Microchip™ (dsPIC30F6014/A) mounted on a custom designed printed circuit board to perform smooth humming control and speech recognition. One DSP is dedicated to speech recognition and implements Hidden Markov Models using dsPIC30F Speech Recognition Library developed by Microchip; the other implements Fast Fourier Transforms on humming signals. The current design has shown that our idea of smooth control not only works, but can be implemented in real time. We have built a prototype, which was implemented and tested on Invacare’s Storm TDX5 (mid-wheel drive power chair) donated to us by East Coast Rehab, LLC.

Chapter 1: Introduction

1.1. Problem Statement

Advancements in today’s technology has greatly affected the life of average people during the past decade, but unfortunately wheelchair users around the world have seen little to no improvement on the commercially available wheelchair controllers [15]. It is estimated that there are about 200 million people worldwide using wheelchairs and in the U.S.A. alone roughly 11000 people are affected by spinal cord injury every year. About 47 percent of those injuries lead to quadriplegia [30]. This growing demand for wheelchairs calls for better advancements for powered wheelchair controllers to better suit the needs of these patients.

The extreme difficulty that patients with severe disabilities have been trained to maneuver a power wheelchair has been described in case studies and subjective evidence suggests the existence of a patient population for whom mobility is severely limited if not impossible given currently available power wheelchair control interfaces. An interesting survey by Hines VA Hospital Rehabilitation Research and Development Center was done among 200 practicing clinicians, asking them to provide information about their patients and to give their impressions of the potential usefulness of a new power wheelchair navigation technology. Significant survey results were [15]:

Clinicians indicated that 9 to 10 percent of patients who receive power wheelchair training find it extremely difficult or impossible to use the wheelchair for activities of daily living [15]. When asked specifically about steering and maneuvering tasks, the percentage of patients reported to find these difficult or impossible jumped to 40%. Eighty-five percent of responding clinicians reported seeing some number of patients each year that cannot use a power wheelchair because they lack the necessary motor skills, strength, or visual acuity. Of these clinicians, 32% (27% of all respondents) reported seeing at least as many patients who cannot use a power wheelchair as who can. According to this survey nearly half of patients unable to control a power wheelchair by conventional methods would benefit from an automated navigation system [15].

We believe these results indicate a need, not for more mechanical and systematic improvement, but for entirely new technologies for supervised autonomous navigation. This chapter surveys today's commercially available controllers to power wheelchair users and then introduces the solution proposed by this thesis to the shortcomings of these products.

1.2. Commercially Available Solutions

There are many types of commercially available controllers for powered wheelchairs such as joystick, push-button, head-array and sip-and-puff controllers. All of these controllers are widely used among wheelchair users with different types of injuries. The main issue with majority these controllers, except sip-and-puff, is that the patient is assumed to have reliable mobility in their bodies.

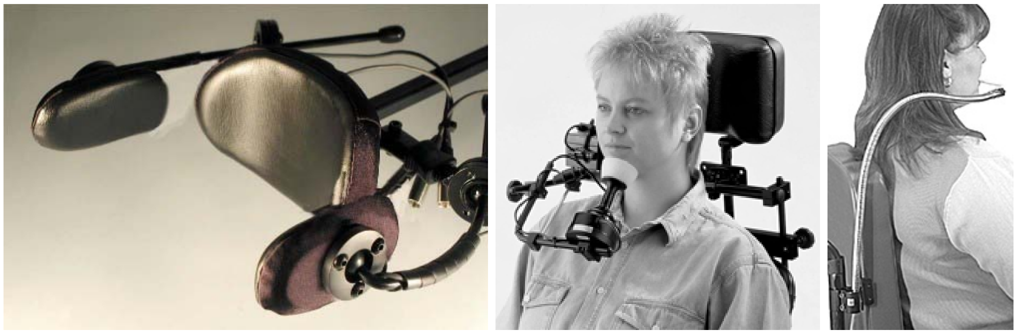

Figure 1. Common Commercially Available Controllers for Powered Wheelchairs

From left to right: head-array, chin and sip-n puff controller. *Source: http://atwiki.assistivetech.net/index.php/Alternative_wheelchair_control*

According to the survey respondents, the vast majority of patients who use a power wheelchair rely on joystick, sip-and-puff, chin, or head-array control interfaces. Very sophisticated control technologies such as eye gaze or tongue pad interfaces are employed by fewer than 5 percent of power wheelchair users (perhaps as few as 1 percent) [2, 15].

Table 1. Break down of power wheelchair control interfaces used in average

Percent of patients using	**Simple Average (n=46)**	**Weighted* Average (n=30)**
Joystick	81	81
Head or chin control	9	9
Sip-and-Puff	6	9
Other: (eye gaze; tongue pad; head, hand, foot switch controls)	4	1
Total	*100*	*100*

* weighted by total number of power wheelchair users reported in survey

Source: http://www.rehab.research.va.gov/jour/00/37/3/fehr.htm

Table 2. Adequacy of existing control interfaces

Measure	Simple Average	Weighted Average
Percentage of patients who: after training, have extreme difficulty using a power wheelchair for daily activities	6	6*
Percentage of patients who: after training, find it impossible to use a power wheelchair for daily activities	4	3*
Total Percentage	*10* *(n=42)*	*9* *(n=38)*
Percent of power wheelchair users who: have difficulty with steering tasks	32	35**
Percent of power wheelchair users for whom: steering tasks are impossible without assistance	9	5**
Total Percentage	*41* *(n=42)*	*40* *(n=38)*

* weighted by numbers trained, reported in survey
** weighted by total number of power wheelchair users reported in survey

Source: http://www.rehab.research.va.gov/jour/00/37/3/fehr.htm

The survey responses summarized in Tables 2 and 3 suggest that the power wheelchair control interfaces used may not, in fact, be adequate to provide truly independent mobility for substantial numbers of persons with disabilities. On average approximately 10 percent of the patients trained to operate a power wheelchair cannot use the chair upon completion of training for daily activities or can do so only with extreme difficulty [15]. Clinicians also indicated that even among their patients who are regular power wheelchair users, 40 percent of these persons have difficulty with steering tasks such as maneuvering the chair throughout the confines of a typical home or office environment, including passage of doorways and entering and exiting elevators. Further, clinicians reported that between five and nine percent of regular power wheelchair users find such tasks impossible without assistance [15].

Table 3. Proportion of patients unable to use a power wheelchair

Measure	Simple Average	Weighted Average
Percentage of patients evaluated annually who: are not candidates for a power wheelchair because they lack requisite motor skills, strength, or visual acuity	18* (n=15)	26** (n=44)
Percentage of these patients who: could benefit from a computer-controlled navigation system	49 (n=49)	44*** (n=45)

* Mean of all responses to the first part of question I.5 given as a percentage
** All responses to question I.5 (percentage or absolute number) weighted by the estimated number of patients seen annually
*** Weighted by responses to questions I.2 and/or I.5.

Source: http://www.rehab.research.va.gov/jour/00/37/3/fehr.htm

With the advancements of microprocessors, significant innovation has occurred in power wheelchair control interfaces, as well as many other areas related to control of assistive technology. In addition to the more common interfaces such as sip-and-puff and chin and head controls, power wheelchair users have available to them such complex control schemes as tongue touch pads and eye gaze systems. Nevertheless, we showed that, in spite of today's sophisticated control interfaces, persons with severe and/or multiple disabilities may yet find it prohibitively difficult to smoothly steer a power wheelchair in typical residential, institutional, or office settings in which maneuvering space is limited. The next section will introduce our solution to a control interface for smooth and precise control of powered wheelchair that can significantly improve these current shortcomings.

1.3. Proposed Solutions

The mentioned survey [15] clearly indicates that individuals with severe disabilities which compromise respiratory drive and/or limit the dexterity of the head and hands have few options for steering a power wheelchair. This notion is further reinforced by the fact that 85 percent of respondents reported evaluating some number of patients annually for whom a power wheelchair is not an option because they cannot control it. Of these clinicians, 32 percent indicated that they evaluate at least as many patients who cannot use a power wheelchair as patients who can. These include persons with high-level spinal cord injury, nervous system diseases, cognitive impairment, and blindness, presumably in conjunction with mobility impairment. One must conclude that, for these persons, no independent mobility options exist at this time. Furthermore this clinical survey provides evidence that existing control technologies may not be entirely adequate even for persons who use a power wheelchair on a regular basis. On average, responding clinicians reported that approximately 40 percent of their patients who use power wheelchairs have difficulty with steering tasks and that between five and nine percent find such tasks impossible without assistance [2, 15].

The solution proposed in this work addresses the issue of smooth control for powered wheelchair users that have limited to no limb movement. In this project we put forward a controller interface that is easy to be added on commercially available controllers, such as joysticks, which would enable the voice control of the wheelchair. Using the Hum-power controller a patient would be able to have a complete control over their powered wheelchair without requiring any limb movement and to address the smooth control of the chair for precise maneuvering a novel idea is implemented in the controller. An issue we encountered in our studies was that when using speech recognition techniques the user is still bounded to have predefined number of speed levels. For example; if the speed ranges from 0% to 100% then it is not convenient or practical to have ten different speed commands for each 10% increments in the speed. Since there is only a set number of voice commands available, an issue would rise with the smoothness of the movement in tight areas or for obstacle avoidance. To address this issue the controller is designed to use and recognize the humming of the patient on their neck to translate their frequency of humming into the desired speed level. Using this new technique it is possible to give a precise and smooth control over the speed of the movement while maneuvering in tight areas.

The Hum-power controller presented in this thesis (Figure 2) operates in two different modes; manual or automatic mode. The precise movement and speed changes are not always required given that in large and clear areas it is easy to maneuver the wheelchair without much effort. Automatic mode will be used in such areas when the patient is traveling a long and open path where a smooth control of the chair is not necessary. On the other hand the manual mode is used to navigate through tense areas such as doorways or narrow corridors where the user requires precise control over the speed of the movement. This mode gives complete control over the movement of the chair with variable speed according to their needs for smoother maneuvering.

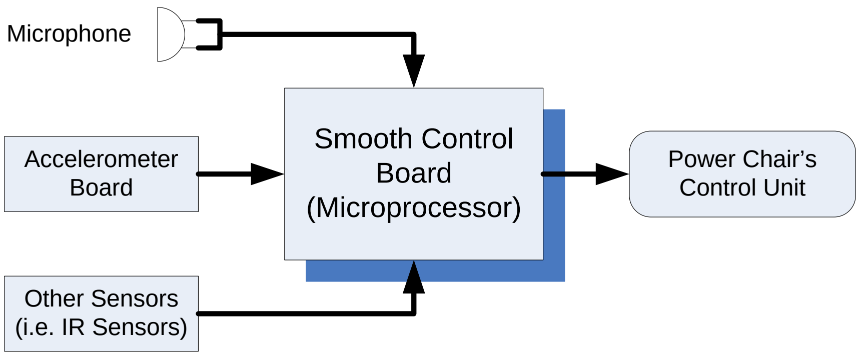
Microphone
Accelerometer Board
Smooth Control Board (Microprocessor)
Power Chair's Control Unit
Other Sensors (i.e. IR Sensors)

Figure 2. Systematic Diagram of Hum-power Controller for Powered Wheelchairs

---

This diagram explores the top-level connection of the main components of this controller. The voice commands are given through the microphone and are recognized by the smooth control board. If the controller is in the manual mode the humming is captured from the neck of the patient with the accelerometer and its frequency is then calculated by the smooth control board which would dictate the speed of the wheelchair. The appropriate control commands are finally given to the power chair's control unit (i.e. joystick.) It is also possible to have sensory inputs such as IR sensors to the control board for obstacle avoidance.

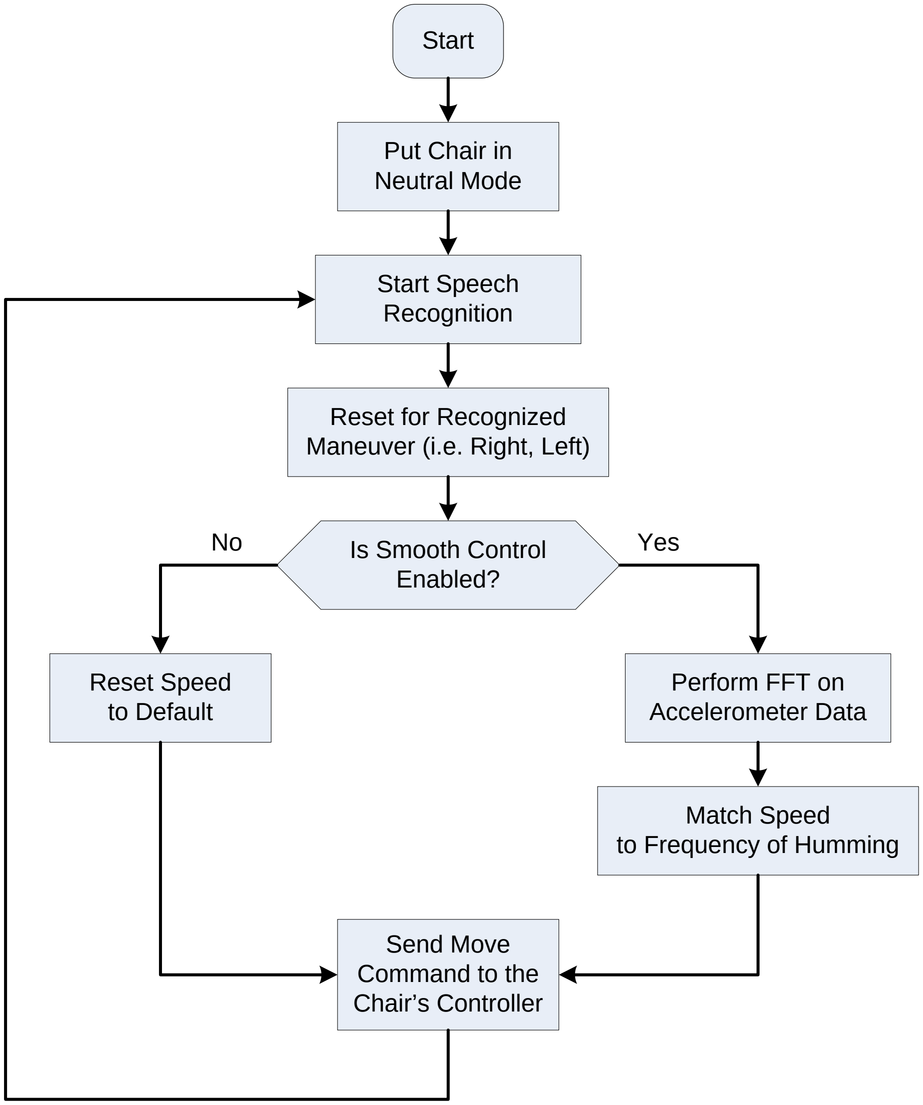
Start
Put Chair in Neutral Mode
Start Speech Recognition
Reset for Recognized Maneuver (i.e. Right, Left)
Is Smooth Control Enabled?
No
Yes
Reset Speed to Default
Perform FFT on Accelerometer Data
Match Speed to Frequency of Humming
Send Move Command to the Chair's Controller

Figure 3. System Flow of the Hum-power Controller for Powered Wheelchairs

This diagram indicates system flow of the operation for the proposed controller. The chair will start in neutral mode and the speech recognition will start listening for the predefined words. To start the operation user will first indicate the control mode. If in manual mode, the smooth control is enabled and the speed of the movement is mapped from the frequency of the humming. Otherwise the speed (initially set to one) is manually set by voice commands.

The designed controller interface in this thesis project uses Hidden Markov Models (HMM) to perform speech recognition on user independent basis for a set number of predefined commands. The patient is able to give four basic commands for direction of movement (right, left, forward and reverse) and if operating in automatic mode a speed change command is also available to change the speed to four preset speed levels (one, two, three and four). The frequency of the humming is calculated using Fast Fourier Transform (FFT) and is mapped to a desired speed of the movement when operating in manual mode. The complete operation instructions for Hum-power controller can be found in the Appendix.

Table 4. Complete List of Voice Commands for Hum-power Controller Interface

Command	Command Description
Control	This is a "Mode" command which starts the manual control of the wheelchair. This command can be given without any prerequisite command at any time and stops the chair resulting in termination of previous mode. After this command is given the user will be prompted for a direction command in which the speed of the movement will be dictated by the frequency of humming.
Go	This is a "Mode" command which starts the automatic control of the wheelchair. This command can be given without any prerequisite command at any time and stops the chair resulting in termination of previous mode. After this command is given the user will be prompted for a direction command in which the initial speed of the movement is set to one. After the wheelchair starts moving the user will be able to change the speed using the Speed command.

Speed	This command is only available in the automatic control mode. Given that the wheelchair is moving at a set speed, if it is desired to change the speed the user gives the Speed command followed by the desired speed number i.e. one, two, three or four.
Stop	This command terminates any operating control mode and stops the wheelchair immediately. After the stop command is given the speech recognition process performs a self test and restarts in a neutral mode.
Forward	This is a direction command that will set the direction of the movement for the wheelchair. It can be given in any control mode but it must be given after either the Control or Go command.
Reverse	This is a direction command that will set the direction of the movement for the wheelchair. It can be given in any control mode but it must be given after either the Control or Go command.
Right	This is a direction command that will set the direction of the movement for the wheelchair. It can be given in any control mode but it must be given after either the Control or Go command.
Left	This is a direction command that will set the direction of the movement for the wheelchair. It can be given in any control mode but it must be given after either the Control or Go command.
One	This is an intensity of speed command. It can only be used in the automatic mode and it must be given after the Speed command. This will set the speed level to 25%.
Two	This is an intensity of speed command. It can only be used in the automatic mode and it must be given after the Speed command. This will set the speed level to 50%.
Three	This is an intensity of speed command. It can only be used in the automatic mode and it must be given after the Speed command. This will set the speed level to 75%.
Four	This is an intensity of speed command. It can only be used in the automatic mode and it must be given after the Speed command. This will set the speed level to 100%.

Other potential solution to the shortcomings of power wheelchair control technologies is to implement automatic and computerized navigation system to assume control of steering if required. A computer-controlled power wheelchair navigation system, which functions in a well-defined but minimally modified environment, has been developed at the University of Notre Dame, Automation and Robotics Laboratory [45-48]. The navigation system has repeatedly demonstrated its ability to guide a power wheelchair along the precise trajectories typically required within a home, office. The long-term goal of this thesis project is to produce a commercially viable product at a reasonable price with indoor/outdoor automated navigation capability and added smooth control facilitation. Such a system would provide persons with severe mobility impairments a degree of autonomy not otherwise possible [46].

Chapter 2: Prototype Development

2.1. MATLAB Environment

i. GMU Neurot

The GMU Neurot was designed to develop a straightforward and effective method for voice recognition which can be easily integrated with the joystick of a powered wheelchair and enable voice control for quadriplegic and disabled individuals. In order to completely control Voice Controlled Wheelchairs (VCWs), only some isolated words need to be recognized (i.e. go, stop, right, left, and backward). The idea and work done for this project was originally designed, implemented, and tested on a robotic arm built with the Lego Mindstorms™ NXT (see figure 4).

This robot is capable of drawing a circle, square, or triangle upon command. It is controlled via USB or Bluetooth connection to a PC; all programming is developed in Matlab™ 7.1 (Mathworks, Natick, MA). The developed voice recognition algorithm yields high accuracy in recognizing the words "triangle", "circle" and "square" with low ambient noise. In this project a method based on cross correlation of mel frequency cepstral coefficients (MFCCs) was used for speech recognition of isolated words. We developed the system and implemented it on three fronts: (1) the robot, (2) computer and robot interface, and (3) voice recognition program.

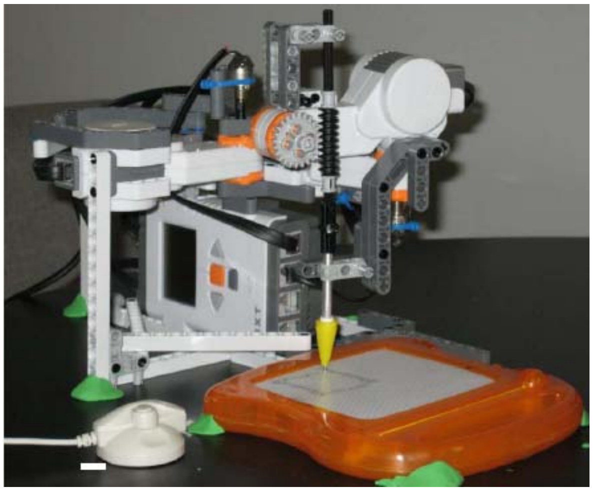

Figure 4. GMU Neurot: The Voice Activated Robotic Arm

Developed using Lego Mindstorms NXT and controlled using Matlab™ . Notice the microphone on the side (lower left), and the self-correcting mechanism for controlling the pressure of the stylus on the magnetic pad. The block with the four buttons contains a 32-bit ARM7 microcontroller. The potentiometers on the motors were secured with the cable ties. Scale: 1cm.

For this process a set of 15 training samples (of 2 second each) was collected in Matlab™ for each command: "circle", "square", and "triangle". The MFCCs of the recorded training sets were calculated and stored in the memory for later comparison. For recognizing the given command the MFCCs of the spoken word is calculated and its coefficients are cross correlated with the ones stored in the memory from the training samples [5]. After comparison of the given command's MFCCs with all 45 MFCCs of the three training sets (corresponding to the three possible words), the computer generates a poll of match and mismatches. The set that has the most matches compared to the others is selected as the recognized word. If there is a tie between the polls or no matches to any of the sets, program declares "no selection" and takes no action. Figure 5 explains the comparison and decision making processes. In the end, after the decision is taken, the degree of confidence on that result is evaluated by dividing the number of matches for that word by the total (15), and multiplying by 100%.

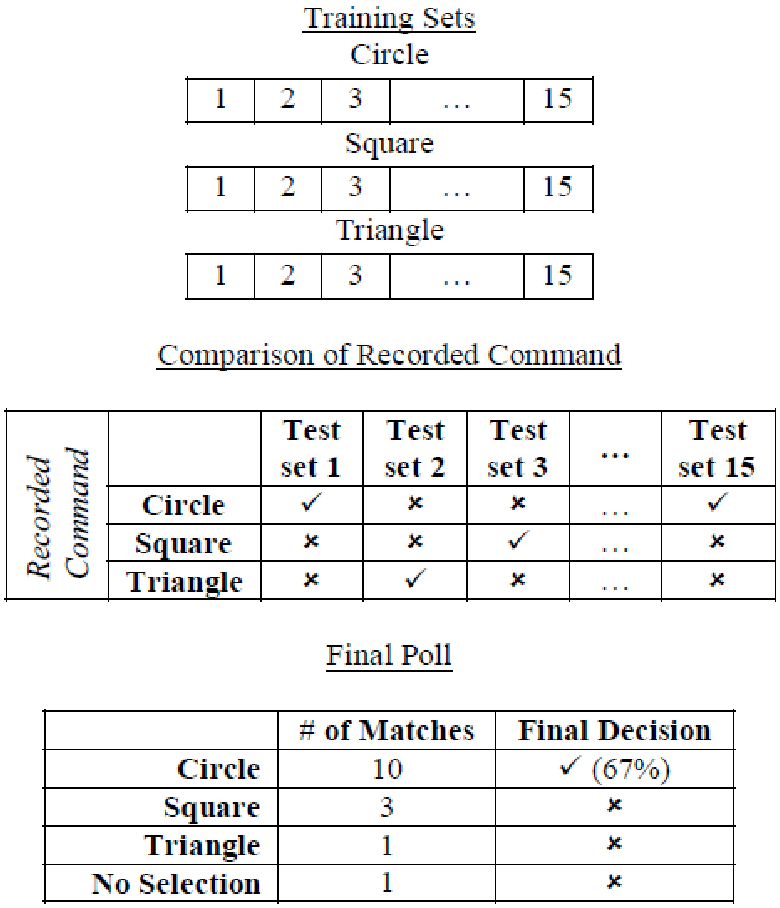

Training Sets

Circle

1	2	3	…	15

Square

1	2	3	…	15

Triangle

1	2	3	…	15

Comparison of Recorded Command

		Test set 1	**Test set 2**	**Test set 3**	**…**	**Test set 15**
Recorded Command	**Circle**	✓	×	×	…	✓
	Square	×	×	✓	…	×
	Triangle	×	✓	×	…	×

Final Poll

	# of Matches	**Final Decision**
Circle	10	✓ (67%)
Square	3	×
Triangle	1	×
No Selection	1	×

Figure 5. Speech Recognition Process Based on MFCC for GMU Neurot

Simple schematic of comparison and decision making process of the proposed method. After polling the three words, if the number of matches with circle was 10, with square was 3, with triangle was 1, and no selection was 1, the degree of confidence would be 67%.

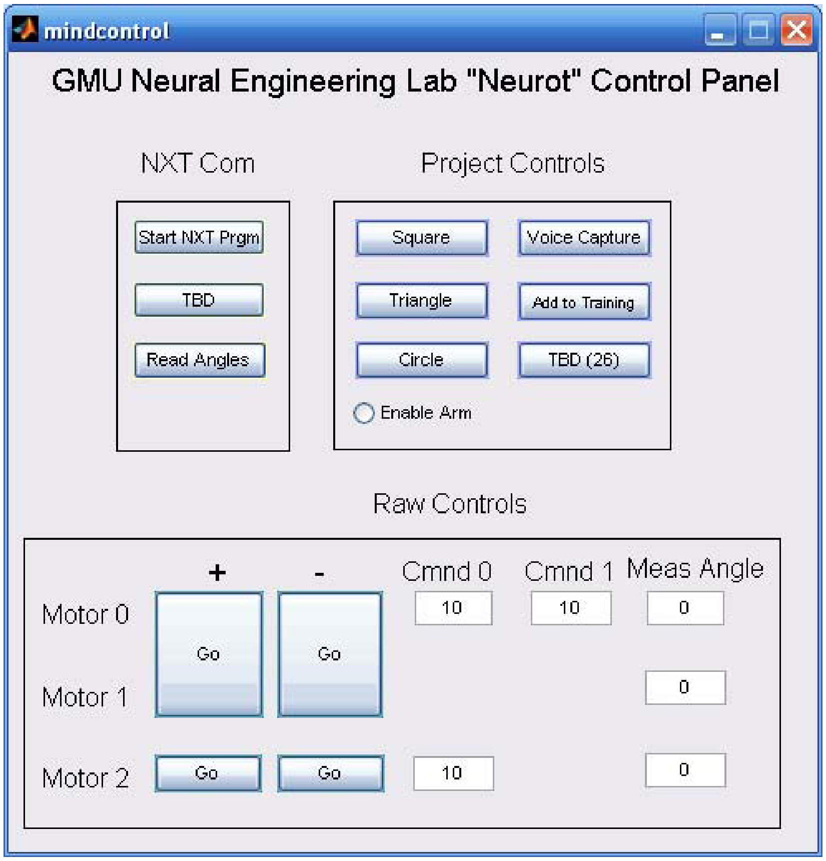

Figure 6. GMU Neurot's Control Panel Computer Interface

Under "raw controls" the user can manually move the robotic arm. With "NXT com" the resident program on the robot can be started, and motor angles are read with a 1 degree precision. "Project Controls" allows for voice capture and manual selection of shape to be drawn. Training set can also be modified with the "add to training" button.

Using the Neurot Control Panel on the computer 15 samples of 2 second recordings are collected for each command (using the Add to Training button in figure 6). 12 cepstral coefficients, excluding the 0'th coefficient, of each sample are calculated and saved as a training instance, part of a training set. Using the Voice Capture button a new command is captured and its 12 cepstral coefficients are calculated and cross correlated with the available training sets. The training set that has the highest cross correlation compared to the others is selected as the spoken word. If there is a tie between the sets or no match to any of the sets the program returns “No Selection” and performs no task.

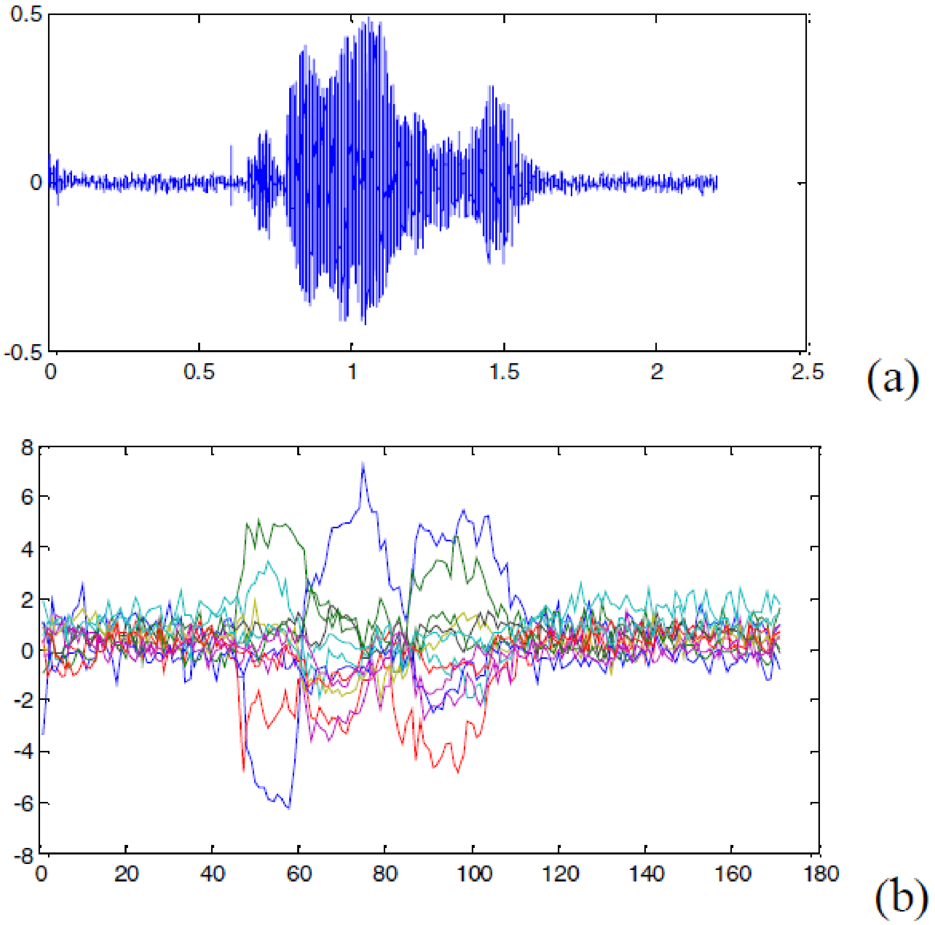

Figure 7. MFCC Representation of Voice Signal

Example of recorded signal for the word triangle (a) and its 12 calculated MFCCs (b). In (a) x axis is given in time (s); in (b) the x axis shows the number of sample frames and the y axis shows the value of mel cepstrum.

The mel frequency bands are positioned logarithmically on the mel scale which approximates the human auditory system's response more closely than the linearly-spaced frequency bands obtained directly from the FFT. To generate the MFCCs of the recorded signals, first their Fourier transform is calculated and then the resulting log amplitude spectrum is mapped onto the Mel scale, using triangular overlapping windows [5]. The Discrete Cosine Transform of the list of Mel log-amplitudes is evaluated as if it were a signal and the MFCCs are the amplitudes of the resulting spectrum (figure 7). The following will explain computation of the MFCCs [5]:

We will use the intelligent sound implementation (ISP) to explain the computation of MFCCs. First the recorded voice is divided into short time windows, where we compute the discrete Fourier transform (DFT) of each time window for the discrete-time signal *x(n)* with length *N*, given by:

$$X(k) = \sum_{n=0}^{N-1} w(n)x(n)e^{\frac{-j2\pi kn}{N}} \quad \textbf{(1)}$$

For $k = 0, 1, \ldots, N-1$, where k corresponds to the frequency $f(k) = kfs/N$, fs is the sampling frequency in Hertz and $w(n)$ is a time window. Here, we chose the Hamming window as a time window, given by $w(n) = 0.54 - 0.46\cos(\pi n/N)$, due to computational simplicity.

The magnitude spectrum $|X(k)|$ is now scaled in both frequency and magnitude. First, the frequency is scaled logarithmically using the Mel filter bank $H(k,m)$ and then the logarithm is taken, yielding:

$$X'(m) = \ln\left(\sum_{k=0}^{N-1} |X(k)|.\, H(k,m)\right)$$

(2)

For $m = 1, 2, \ldots, M$, where M is the number of filter banks and $M \ll N$. The Mel filter bank is a collection of triangular filters defined by the center frequencies $f_c(m)$, written as:

$$H(k,m) = \begin{cases} 0 & for \quad f(k) < f_c(m-1) \\ \dfrac{f(k) - f_c(m-1)}{f_c(m) - f_c(m-1)} & for \quad f_c(m-1) \le f(k) < f_c(m) \\ \dfrac{f(k) - f_c(m+1)}{f_c(m) - f_c(m+1)} & for \quad f_c(m) \le f(k) < f_c(m+1) \\ 0 & for \quad f(k) \ge f_c(m+1) \end{cases}$$

(3)

The center frequencies of the filter bank are computed by approximating the Mel scale with:

$$\phi = 2595 \log_{10}\left(\frac{f}{700} + 1\right)$$

(4)

which is a common approximation. Note that this equation is non-linear for all frequencies. Then a fixed frequency resolution in the Mel scale is computed, corresponding to a logarithmic scaling of the repetition frequency, using $\Delta\phi = (\phi_{max} - \phi_{min}) / (M + 1)$ where ϕ_{max} is the highest frequency of the filter bank on theMel scale, computed from f_{max} using the equation (4), ϕ_{min} is the lowest frequency in Mel scale, having a corresponding f_{min}, and M is the number of filter banks. The center frequencies on the Mel scale are given by $\phi_c(m) = m \cdot \Delta\phi$ for $m = 1, 2, . . . ,M$. To obtain the center frequencies in Hertz, we apply the inverse of equation (4), given by:

$$f_c(m) = 700 \cdot \left(10^{\frac{\phi_c(m)}{2595}} - 1\right) \qquad \textbf{(5)}$$

which are inserted into equation (3) to give the Mel filter bank. Finally, the MFCCs are obtained by computing the discrete cosine transform (DCT) of $X'(m)$ using:

$$c(l) = \sum_{m=1}^{M} X'(m) \cdot \cos\left(l \frac{\pi}{M}\left(m - \frac{1}{2}\right)\right) \qquad \textbf{(6)}$$

for $l = 1, 2, . . . ,M$, where $c(l)$ is the l^{th} MFCC.

The MFCCs of the spoken command are compared with the ones in the training sets via cross correlation. When two sets of MFCCs are cross correlated with each other the result is a set twice the size of the original sets with multiple possible peaks at the center. If the signals are somewhat similar a relatively large peak is distinguished at the center of the signal. While comparing the cross correlation of the recorded command to the training set in each test the largest peak produced by the cross correlation with circle, square and triangle are compared with each other and the one with the largest peak is taken as the spoken word. Figure 8 shows the result of one test done with the sample test. They are the largest peak resulted from the cross correlation of MFCCs from triangle with circle, square and triangle. It is observed that the cross correlation of MFCCs of word triangle with triangle produces a larger peak compared to the cross correlation with circle and square.

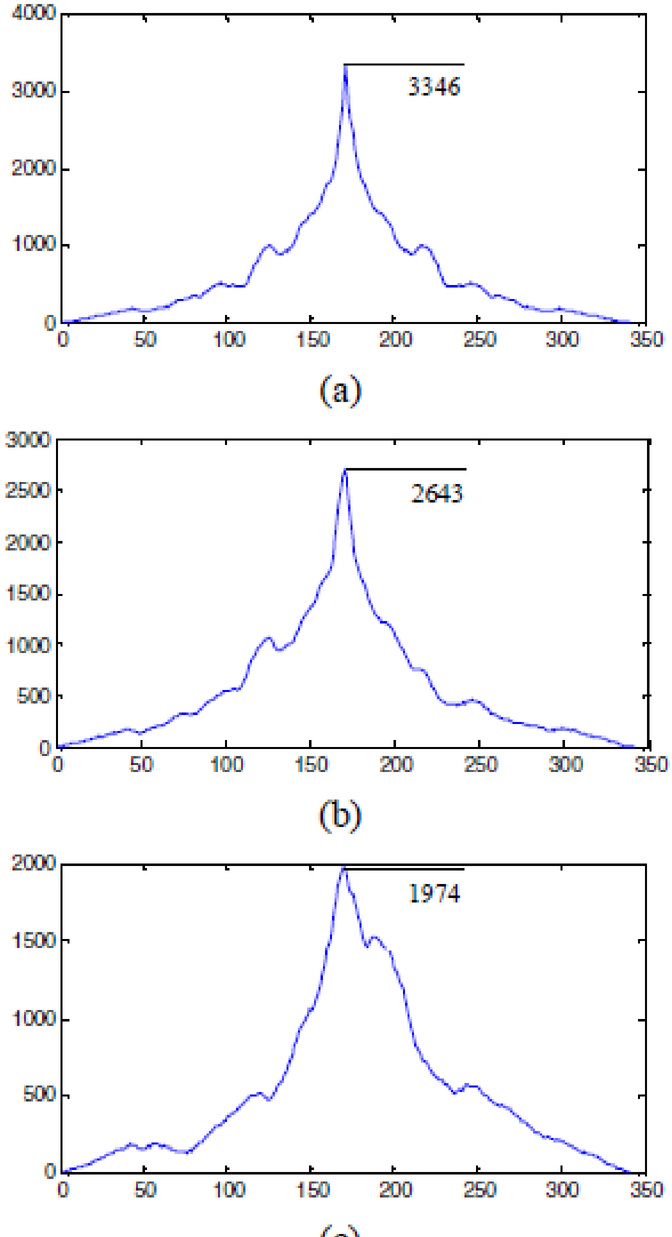

(a)

(b)

(c)

Figure 8. Cross Correlation Results for the MFCC's of Different Words

---

Resulting cross correlation of MFCCs of a test word (in this case “triangle”) with example training words (a) triangle, (b) circle, (c) square. It can be observed that the highest peak is obtained when the words are identical (a), but as the words are different from triangle the peak clearly has a lower amplitude (b & c).

This method was tested by several speakers in our laboratories. We present here the results for a single male speaker. The algorithm was evaluated in a low ambient noise environment by the same speaker. The algorithm was tested for a total of 100 times, where each command was spoken 25 times and for the last 25 times noise and other words were used to check “No Selection” feature of the system. This particular test resulted in 99% accuracy; numerical results are shown in table 5.

Table 5. Accuracy of MFCC based speech recognition for GMU Neurot

Spoken Word	**# of Matches to**				**Accuracy**
	Circle	*Square*	*Triangle*	*NS*	
Circle	24	1	0	0	96%
Square	0	25	0	0	100%
Triangle	0	0	25	0	100%
*NS**	0	0	0	25	100%

* NS = No Selection

2.2. LabVIEW Environment

Speech recognition for powered wheelchairs was farther tested and analyzed using different projects utilizing the Microsoft’s Speech SDK 5.1 in LabVIEW environment. Speech SDK 5.1 by Microsoft features great set of The Speech Application Programming Interface (SAPI) for speech recognition and speech synthesis within Windows applications.

i. Voice Activated RC Car

The voice activated RC car was a simple startup project for testing and familiarizing with the speech SDK. In this project the RF controller of the RC car was interfaced to the computer using transistor switches operated by digital outputs of a data acquisition device (DAQ) from National Instruments (NI). The user interface of the program showed the recognized word and then turned on/off the appropriate switch for the task requested. This project was successfully tested and showed that the SAPIs are easily integrated with LabVIEW. The computer would continuously listen for the words spoken into the microphone and a word recognized matched the predefined word set it would perform the corresponding action. In this project the user was required to say the keywords of “Start Listening” for the computer start the program and could perform movements of right, left, back and forward by saying the word command. To turn off the process keywords of “Stop Listening” could be given to prevent the program from accidental word matching.

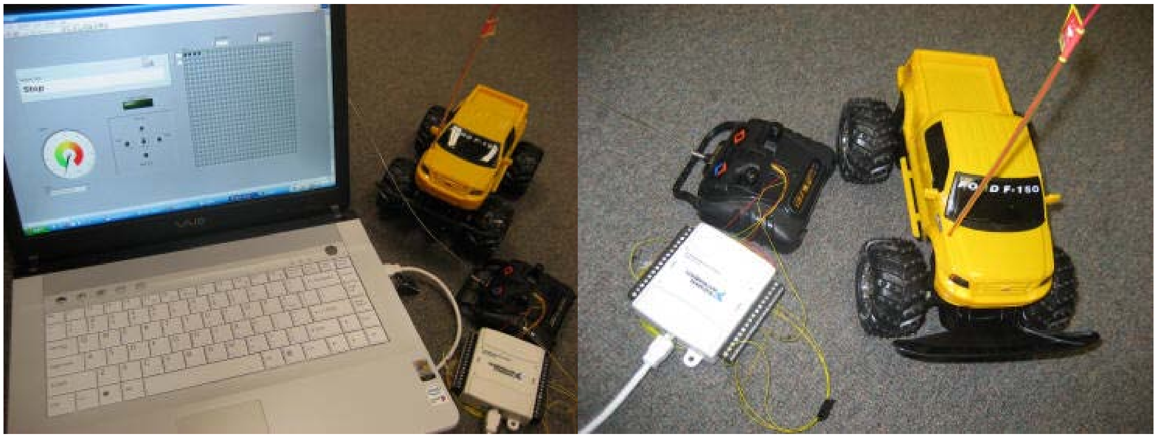

Figure 9. Voice Activated RC Car Using LabVIEW

The RC car controlled via LabVIEW and NI-DAQ via voice commands. The program running on the computer utilizes the Microsoft’s Speech SDK 5.1 for speech recognition and performs the required actions by controlling the switches attached to the physical controls of the RC car’s RF controller.

ii. Voice Activated Mini Lego Chair

Using Lego Mindstorms™ NXT a simple replica of a power chair was designed which was equipped with two proximity sensors. The goal of this project was to farther test the speech recognition capabilities for voice control of the chair and to examine the obstacle avoidance possibilities for the future work. Since the Mindstorms' NXT is Bluetooth enabled the control commands for this project were sent via Bluetooth partnership with the computer. The program designed in LabVIEW made use of Microsoft's Speech SDK 5.1 for speech recognition and monitored the proximity sensors for obstacle avoidance. This project was successfully implemented and the chair was able to stop before striking the presented obstacles.

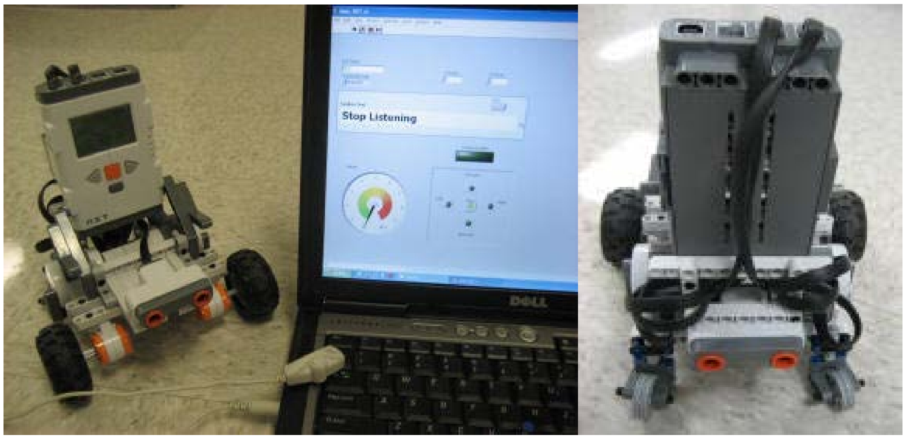

Figure 10. Voice Activated Mini Lego Chair Using LabVIEW

The Mini Lego chair designed using Lego Mindstorms™ NXT was voice controlled via Bluetooth communications. The LabVIEW program running on the computer used Microsoft Speech SDK 5.1 for speech recognition and communicated the commands to the Mini Chair using Bluetooth. The chair was capable of obstacle avoidance using its two front and back proximity sensors.

Chapter 3: Microcontroller Implementation for Wheelchair

3.1. Evaluation Board

The dsPICDEM™ 1.1 plus evaluation board (see figure 11) was used for initial stages of microcontroller implementation of smooth control for powered wheelchair. The dsPICDEM™ 1.1 Plus Development Board Kit serves as a development and evaluation tool for dsPIC30F/33F High Performance Digital Signal Controllers and PIC24H/24FPIC® microcontrollers. This board made available by Microchip provides the application designers with a low cost development tool to become familiar with the dsPIC30F/33F and PIC24H 16-bit architecture, high performance peripherals and powerful instruction set. The board features an active demonstration program loaded on the installed dsPIC30F6014A device. Several program functions are selectable via a menu system displayed on the LCD. These include: temperature and voltage measurements, frequency domain characteristics of a sine wave signal generated on-board from a digital potentiometer, FIR and IIR digital filter selections and DTMF tone generation using the Codec interface peripheral.

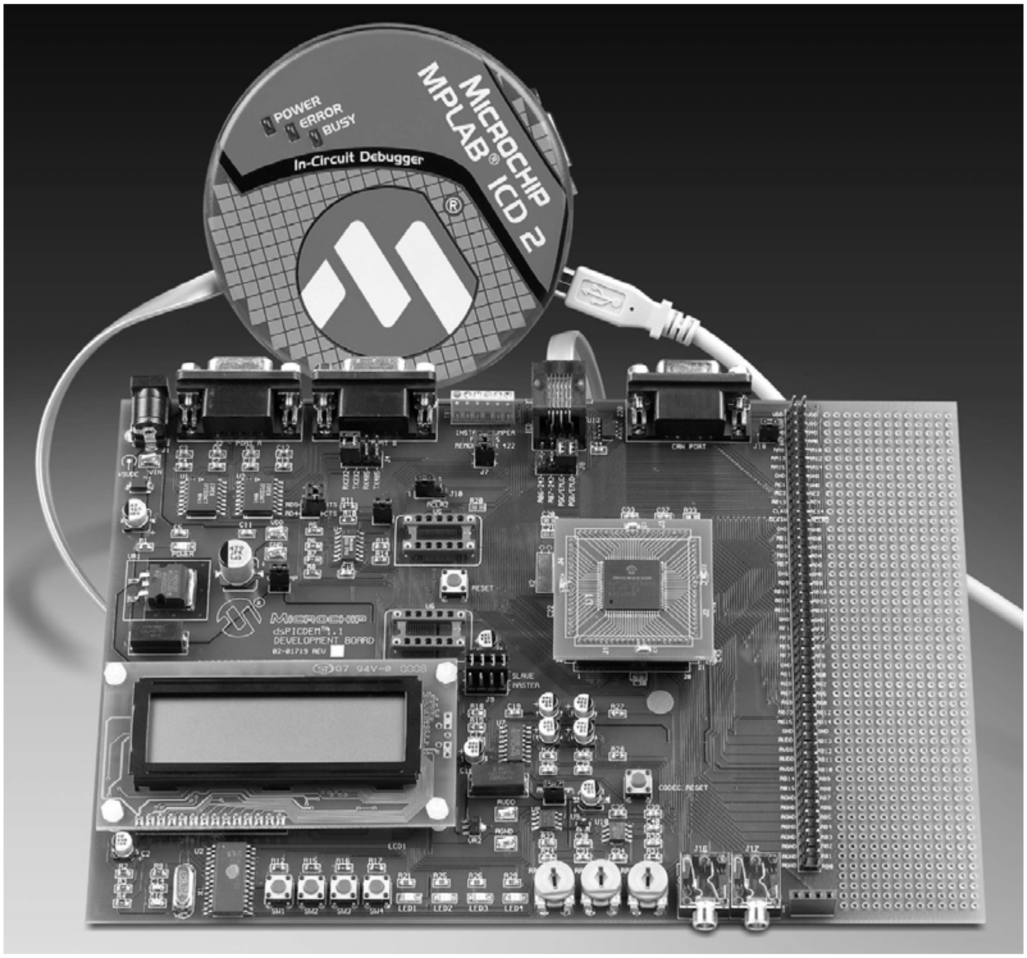

Figure 11. The dsPICDEM™ Plus Development Board with MPLAB ICD 2

> The dsPICDEM™ 1.1 Plus Development Board Kit serves as a development and evaluation tool for dsPIC30F/33F High Performance Digital Signal Controllers and PIC24H/24F PIC® microcontrollers.

The dsPICDEM™ 1.1 Plus Development Board has separate on-board +5V and +3.3V regulators for VDD and AVDD with direct input from 9V, AC/DC wall adapter. This board supports full onboard programming and debugging features with interfacing to MPLAB ICD 2 Debugger/Programmer and includes a pad location for 80-pin TQFP dsPIC DSC devices. The board includes multiple serial communication channels such as two RS-232 communication channels, 6-pin terminal block and configuration jumper for RS-485 and RS-422 communication on UART1 from the dsPIC DSC device and a single CAN communication channel. This board also houses a 122 x 32 dot addressable LCD controlled via PIC18F242 LCD controller.

The Voice Band Codec integrated with this board was one of the primary reasons for choosing this evaluation board. A Si3000 Voice band Codec chip is included with a jumper for selection of master or slave modes. An optional clock oscillator for Si3000 Voice band Codec can also be used for related applications. There is a 4-pin header for the Codec Line In and Line Out with one 3.5 mm phono jack for the Codec left and right speaker outputs and one 3.5 mm phono jack for the Codec MIC input.

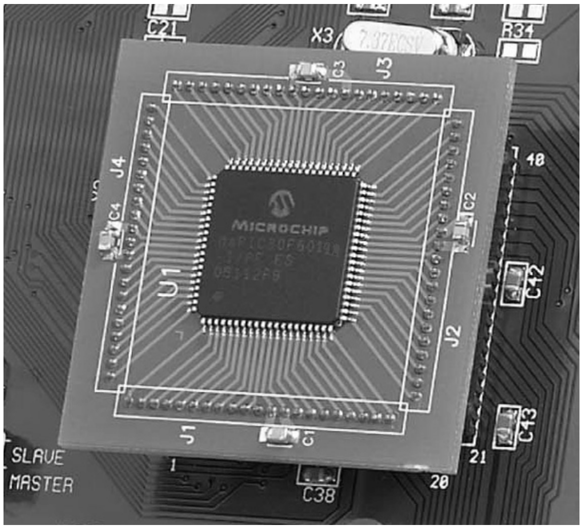

Figure 12. dsPIC30F6014A Plug-in Module

The dsPIC30F6014A PIM is designed to demonstrate the capabilities of the dsPIC30F6014A family of devices using an 80-pin PIM interface. The dsPIC30F6014A is a high-performance 16-bit Digital Signal Controller in an 80-pin TQFP package.

Initial programming and testing was done on the dsPICDEM™ 1.1 Plus Development Board with the dsPIC30F6014A plug-in module (see figure 12). The dsPIC30F6014A plug-in module (PIM) is designed to demonstrate the capabilities of the dsPIC30F6014A family of devices using an 80-pin PIM interface. The dsPIC30F6014A is a high-performance 16-bit Digital Signal Controller in an 80-pin TQFP package. Next section will cover necessary information about this microcontroller.

3.2. dsPIC30F Microcontroller

The dsPIC30F6014 was used as the microcontroller for this project. The dsPIC30F CPU module has a 16-bit (data) modified Harvard architecture with an enhanced instruction set, including significant support for DSP. The CPU has a 24-bit instruction word, with a variable length opcode field. The program counter (PC) is 24-bits wide and addresses up to 4M x 24 bits of user program memory space. A single cycle instruction pre-fetch mechanism is used to help maintain throughput and provides predictable execution. All instructions execute in a single cycle, with the exception of instructions that change the program flow, the double-word move (MOV.D) instruction and the table instructions. Overhead free program loop constructs are supported using the DO and REPEAT instructions, both of which are interruptible at any point.

The dsPIC30F devices have sixteen 16-bit working registers in the programmer's model. Each of the working registers can act as a data, address, or address offset register. The 16th working register (W15) operates as a software stack pointer for interrupts and calls. The dsPIC30F instruction set has two classes of instructions: the MCU class of instructions and the DSP class of instructions. These two instruction classes are seamlessly integrated into the architecture and execute from a single execution unit. The instruction set includes many addressing modes and was designed for optimum C compiler efficiency.

The data space can be addressed as 32K words or 64 Kbytes and is split into two blocks, referred to as X and Y data memory. Each memory block has its own independent Address Generation Unit (AGU). The MCU class of instructions operates solely through the X memory AGU, which accesses the entire memory map as one linear data space. Certain DSP instructions operate through the X and Y AGUs to support dual operand reads, which splits the data address space into two parts. The X and Y data space boundary is device specific. The upper 32 Kbytes of the data space memory map can optionally be mapped into program space at any 16K program word boundary defined by the 8-bit Program Space Visibility Page (PSVPAG) register. The program to data space mapping feature lets any instruction access program space as if it were data space. Furthermore, RAM may be connected to the program memory bus on devices with an external bus and used to extend the internal data RAM.

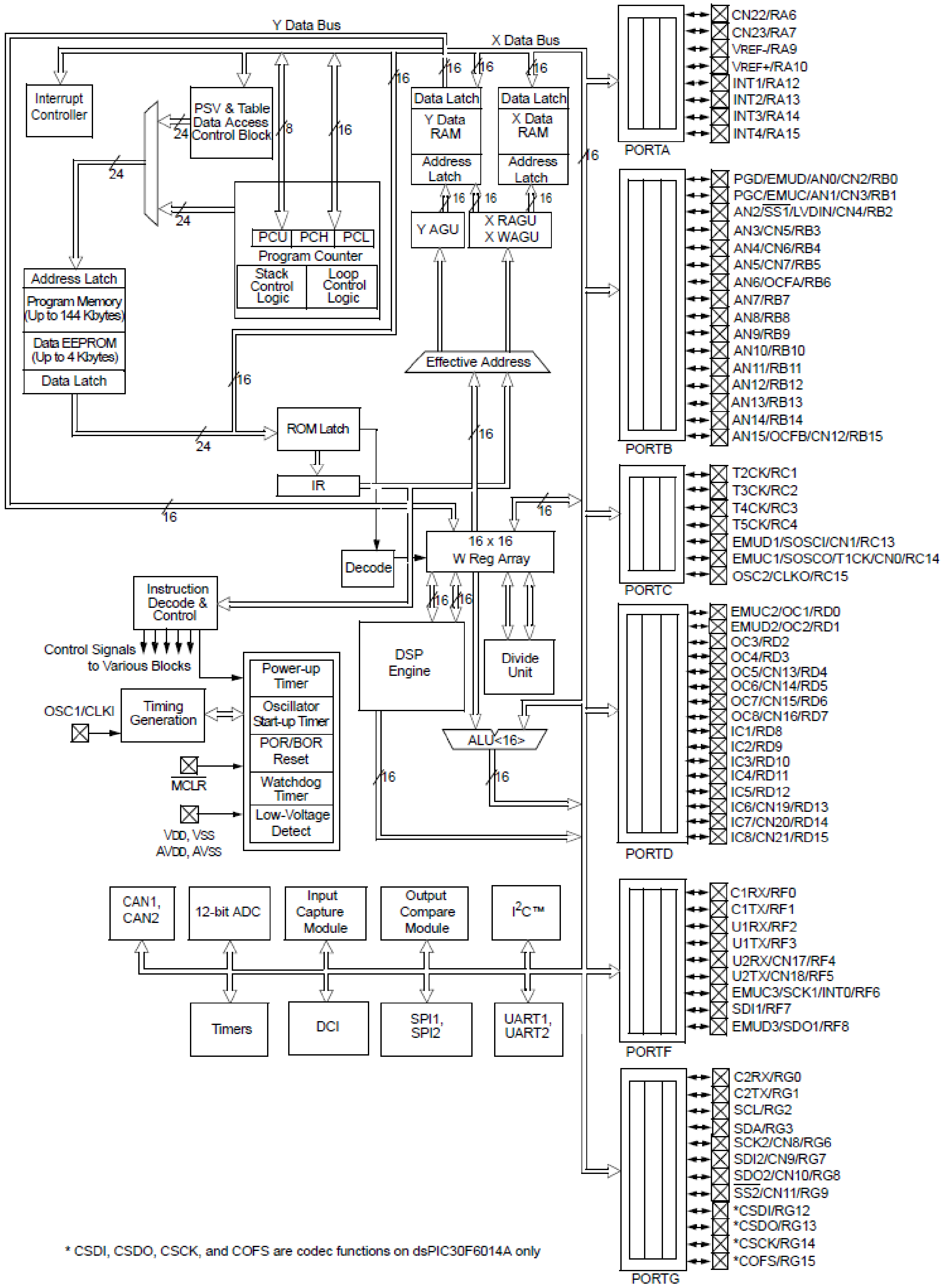

* CSDI, CSDO, CSCK, and COFS are codec functions on dsPIC30F6014A only

Figure 13. The dsPIC30F6014A Block Diagram

Overhead free circular buffers (modulo addressing) are supported in both X and Y address spaces. The modulo addressing removes the software boundary checking overhead for DSP algorithms. Furthermore, the X AGU circular addressing can be used with any of the MCU class of instructions. The X AGU also supports bit-reverse addressing to greatly simplify input or output data reordering for radix-2 FFT algorithms.

The CPU supports Inherent (no operand), Relative, Literal, Memory Direct, Register Direct and Register Indirect Addressing modes. Each instruction is associated with a predefined addressing mode group depending upon its functional requirements. As many as 6 addressing modes are supported for each instruction. For most instructions, the dsPIC30F is capable of executing a data (or program data) memory read, a working register (data) read, a data memory write and a program (instruction) memory read per instruction cycle. As a result, 3 operand instructions can be supported, allowing A+B=C operations to be executed in a single cycle.

The DSP engine features a high speed, 17-bit by 17-bit multiplier, a 40-bit ALU, two 40-bit saturating accumulators and a 40-bit bi-directional barrel shifter. The barrel shifter is capable of shifting a 40-bit value up to 15 bits right, or up to 16 bits left, in a single cycle. The DSP instructions operate seamlessly with all other instructions and have been designed for optimal real-time performance. The MAC instruction and other associated instructions can concurrently fetch two data operands from memory while multiplying two W registers. This requires that the data space be split for these instructions and linear for all others. This is achieved in a transparent and flexible manner through dedicating certain working registers to each address space. The dsPIC30F has a vectored exception scheme with up to 8 sources of non-maskable traps and 54 interrupt sources. Each interrupt source can be assigned to one of seven priority levels.

3.3. Designed Board

i. Speech Recognition Engine

The dsPIC30F Speech Recognition Library was used as the speech recognition engine of this project. The dsPIC30F Speech Recognition Library allows the incorporation of speech recognition in an embedded application program running on a dsPIC30F device. A predefined list of words controls the application with only a modest amount of RAM and program memory. The word list is created with the dsPIC30F Speech Recognition Library Word Library Builder. The Word Library Builder is a PC-based program that lets users select and implement the user interface vocabulary. The Word Library Builder provides the supplemental files needed by the user application to define the allowable words, the Library Keyword, the word recognition features for the Vector Codebook and the Hidden Markov Model (HMM) data files for each library word. The dsPIC30F Speech Recognition Library provides an audio interface to a user's application program, allowing the user to control the application by uttering discrete words that are contained in a predefined word library. The words chosen for the library are specifically relevant to the interaction between the application program and the user. Upon recognition of a word, the application program takes an appropriate action as shown in figure 14.

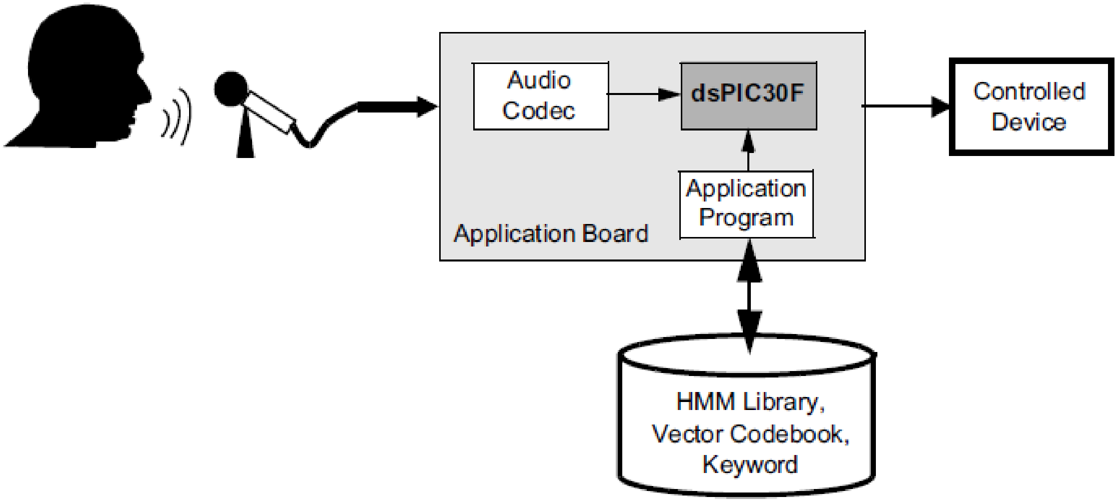

Figure 14. Overview of Speech Recognition

> The Speech Recognition Library provides isolated, speaker independent word recognition of US English. It allows a user to control an application through a set of fixed, voice commands. The library has already been pre-trained by a demographic cross-section of male and female US English speakers. Conveniently, no training is required for end-users of the product.

The dsPIC30F Speech Recognition Library uses a recognition algorithm based on discrete Hidden Markov Model (HMM) of words (one HMM model for each word in an application word library). A word spoken through a microphone connected to the dsPIC30F application board is analyzed on a frame-by-frame basis using RASTA-PLP algorithm and quantized into feature vectors of sound characteristics against a vector codebook. The quantized feature vectors are then examined to determine what word HMM model they most closely match. The dsPIC30F Speech Recognition Library operates in both clear (free of noise) and noisy conditions. Background interference can include white noise, office noise and passenger compartment noise components in any mixture. Total signal-to-noise ratio (SNR) should be no less than 15 dB. A signal level above the noise threshold is presumed to be an incoming word.

The dsPIC30F Speech Recognition Library can operate with a word library of up to 100 words. The word library is built around a keyword that is readily interpreted. Depending on the operating mode used, this keyword can be used to self-test the library and to trigger a recognition session. Successful recognition requires the words to be separated by a pause of at least one-half second but less than some specified period (normally programmed for five seconds). After a pause that times out, a new recognition session must be started. Optionally, the operating mode can be set to disable self-testing and/or keyword activation. When keyword activation is disabled, there is no timeout. Words must only be separated by at least 500 milliseconds.

Figure 15 is a simplified flow diagram of the dsPIC30F Speech Recognition Library operation. When the application board is powered up, the library is initialized, which also establishes the operating mode. The operating mode determines if a self-test is run and if the keyword is used to activate a recognition session. The self-test processes a sample utterance (stored in memory) of the library keyword. If the self-test fails, the diagnostic routine returns an error code indicating that appropriate remedial action must be taken. For example, it may be necessary to verify the build of the application. If the self-test is successful, the library estimates a baseline noise level and enters either the Keyword Search mode or the Listen mode, depending on whether keyword activation is enabled.

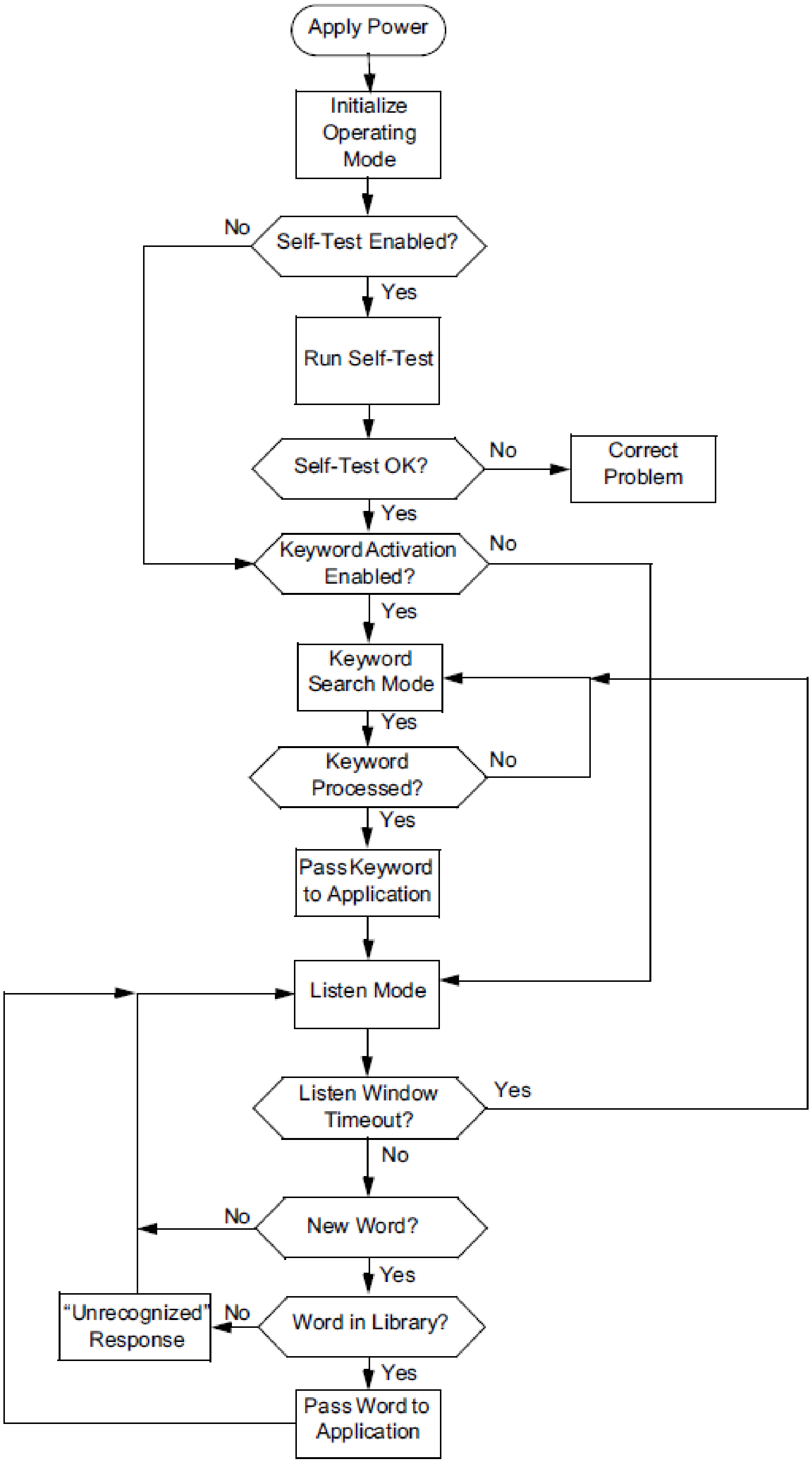

Figure 15. Overview of Speech Recognition Flow Diagram

If keyword activation is enabled, the library remains in the Keyword Search mode until the user articulates the keyword. In this mode, the keyword must be recognized before any further speech recognition can take place. This functionality is important in applications where user security is an issue. For example, a user might be required to articulate a specific word such as “security” followed by a series of numbers to gain access to something. Once the keyword is recognized, the library enters the Listen mode. In this mode the library must receive a new word within the specified Listen Window timeout period (normally about 5 seconds). If the timeout period elapses without a new word, and keyword activation is enabled, the library reverts to the Keyword Search mode. The user must then rearticulate the keyword to start a new recognition session. If keyword activation is not enabled, the library immediately enters the Listen mode. In this mode, the library attempts to recognize any incoming word. Upon successful recognition of the first word, the library notifies the user application and listens for the next word.

ii. Humming Detection Technique

The innovative way of control in this project through humming required the detection of humming frequency and for this matter a small board equipped with an accelerometer was designed to pick up the vibration due to the humming. Figure 16 shows the designed board with the accelerometer. The analog output of this accelerometer was captured using the dsPIC and converted to digital signals. Using a set of 512 samples from these data points the frequency of humming is established using Fast Fourier Transform (FFT).

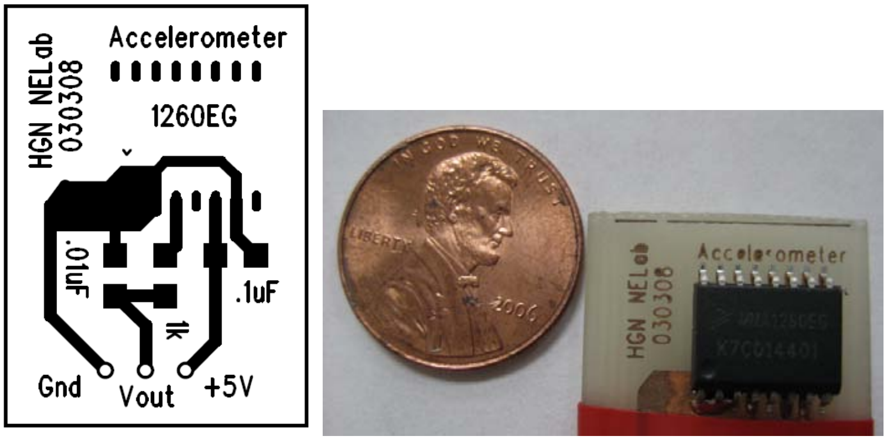

Figure 16. Hum Detection Board

Humming detection board equipped with MMA1260EG Low G Micromachined Accelerometer. This board is placed on the neck of the user and is used to monitor and record vibrations due to humming. The vibration recorded via this board is analyzed using FFT technique to find the frequency of humming which is then translated into the desired speed for the chair.

Microchip's 16-bit dsPIC® Digital Signal Controllers feature a DSP Engine in the CPU that is capable of executing FFT with great efficiency (high speed and low RAM usage). The on-chip features enabling the FFT implementation include; bit-reversed addressing, Multiply-accumulate (MAC) type instructions and the ability to store and retrieve constants stored in program memory. Microchip provides a DSP functions library that provides in-place FFT functions. In this project the vibrations picked up by the humming detection board are recorded and analyzed. The general form of the detected vibration is of a simple sinusoidal signal where after performing FFT produces a frequency bin with a single bin having the highest magnitude representing the frequency of the vibration (see figure 17).

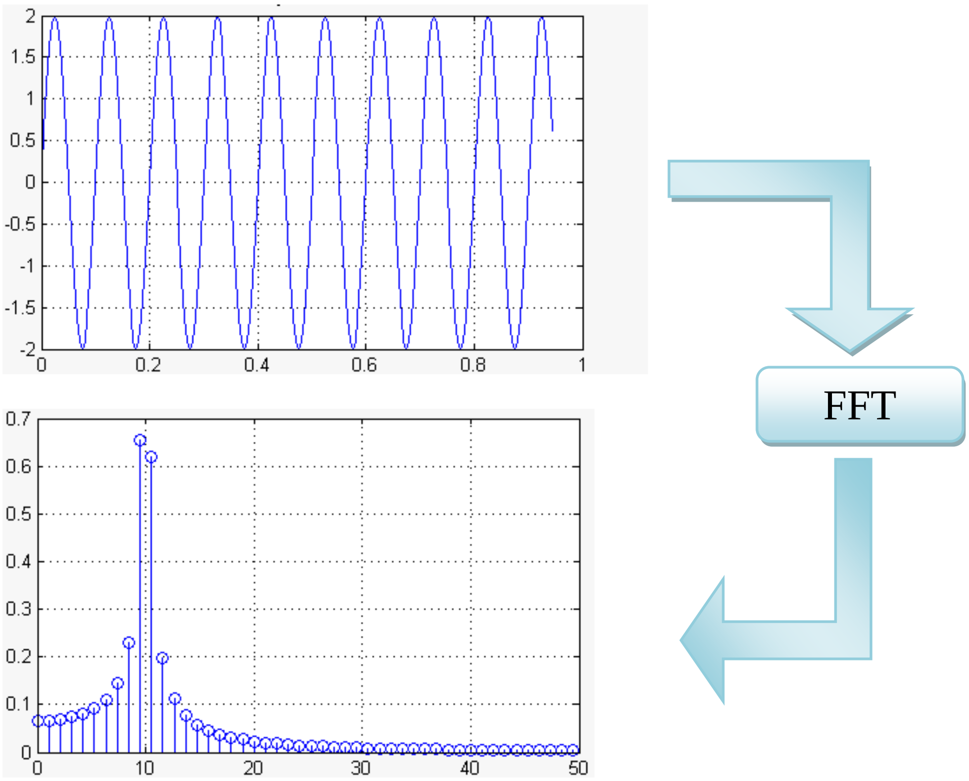

Figure 17. Fast Fourier Transform

The vibration recorded via the humming detection board is of the sinusoidal signal represented in the top graph. This signal is then fed and stored into the DSP for frequency analysis. After performing the FFT analysis on this signal a set of frequency bins are created that indicate the frequency of the recorded signal. The bin with the highest magnitude represents the frequency of the signal (bottom graph).

The FFT is done in complex notation where the time and frequency domains each contain one signal made up of *N* complex points. Each of these complex points is composed of two numbers, the real part and the imaginary part. In other words, each complex variable holds two numbers. The FFT operates by decomposing an *N* point time domain signal into *N* time domain signals each composed of a single point. The second step is to calculate the *N* frequency spectra corresponding to these *N* time domain signals.

Lastly, the *N* spectra are synthesized into a single frequency spectrum. Figure 18 shows an example of the time domain decomposition used in the FFT [49].

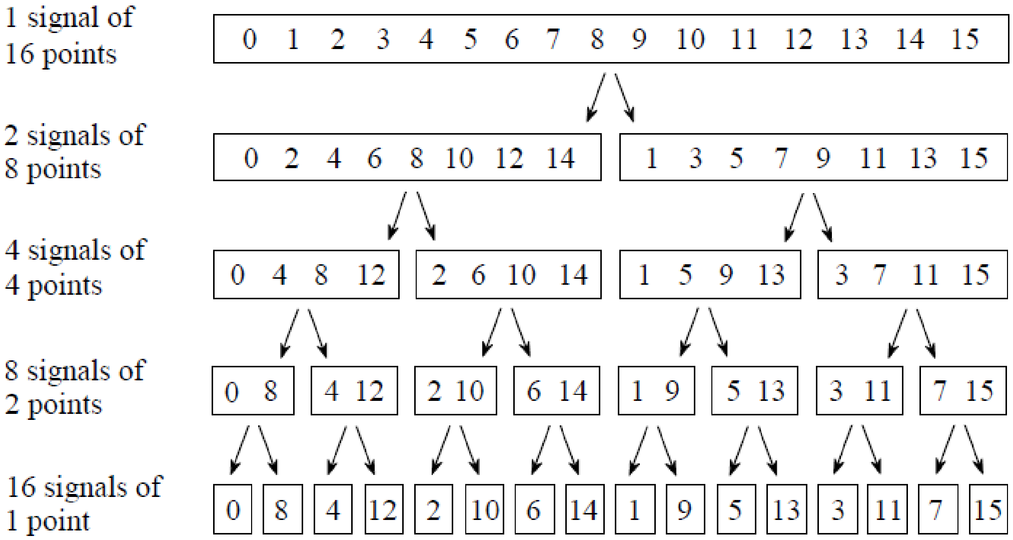

Figure 18. The FFT Decomposition

An N point signal is decomposed into N signals each containing a single point. Each stage uses an interlace decomposition, separating the even and odd numbered samples. In this example, a 16 point signal is decomposed through four separate stages. The first stage breaks the 16 point signal into two signals each consisting of 8 points. The second stage decomposes the data into four signals of 4 points. This pattern continues until there are N signals composed of a single point. An interlaced decomposition is used each time a signal is broken in two, that is, the signal is separated into its even and odd numbered samples. There are Log_2N stages required in this decomposition, i.e., a 16 point signal (2^4) requires 4 stages, a 512 point signal (2^7) requires 7 stages, a 4096 point signal (2^{12}) requires 12 stages, etc.
Source: http://www.dspguide.com/ch12/2.htm

The decomposition is nothing more than a reordering of the samples in the signal. Figure 19 shows the rearrangement pattern required. On the left, the sample numbers of the original signal are listed along with their binary equivalents. On the right, the rearranged sample numbers are listed, also along with their binary equivalents. The important idea is that the binary numbers are the reversals of each other [49]. For example, sample 3 (0011) is exchanged with sample number 12 (1100). Likewise, sample number 14 (1110) is swapped with sample number 7 (0111), and so forth. The FFT time domain decomposition in the dsPIC is carried out by a bit reversal sorting algorithm. This involves rearranging the order of the N time domain samples by counting in binary with the bits flipped left-for-right (far right column in figure 19).

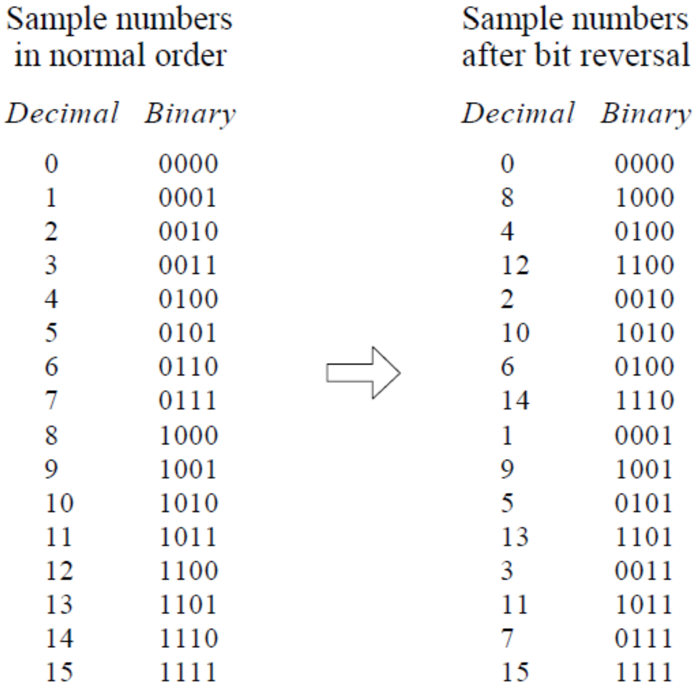

Sample numbers in normal order			Sample numbers after bit reversal	
Decimal	*Binary*		*Decimal*	*Binary*
0	0000		0	0000
1	0001		8	1000
2	0010		4	0100
3	0011		12	1100
4	0100		2	0010
5	0101		10	1010
6	0110	⇨	6	0100
7	0111		14	1110
8	1000		1	0001
9	1001		9	1001
10	1010		5	0101
11	1011		13	1101
12	1100		3	0011
13	1101		11	1011
14	1110		7	0111
15	1111		15	1111

Figure 19. The FFT Bit Reversal Sorting

The FFT time domain decomposition can be implemented by sorting the samples according to bit reversed order. This involves rearranging the order of the N time domain samples by counting in binary with the bits flipped left-for-right (such as in the far right column).

Source: http://www.dspguide.com/ch12/2.htm

The next step in the FFT algorithm is to find the frequency spectra of the 1 point time domain signals, which is equal to itself. This means that nothing is required to do this step, but each of the 1 point signals is now a frequency spectrum, and not a time domain signal [46]. The last step in the FFT is to combine the N frequency spectra in the exact reverse order that the time domain decomposition took place. In the first stage, 16 frequency spectra (1 point each) are synthesized into 8 frequency spectra (2 points each). In the second stage, the 8 frequency spectra (2 points each) are synthesized into 4 frequency spectra (4 points each), and so on. The last stage results in the output of the FFT, a 16 point frequency spectrum.

Figure 20 shows the structure of the entire FFT process used in the dsPIC. The time domain decomposition is accomplished with a bit reversal sorting algorithm. Transforming the decomposed data into the frequency domain involves nothing and therefore does not appear in the figure. The frequency domain synthesis requires three loops. The outer loop runs through the Log_2N stages (i.e., each level in figure 18, starting from the bottom and moving to the top). The middle loop moves through each of the individual frequency spectra in the stage being worked on (i.e., each of the boxes on any one level in figure 18). The innermost loop uses the butterfly to calculate the points in each frequency spectra (i.e., looping through the samples inside any one box in figure 18).

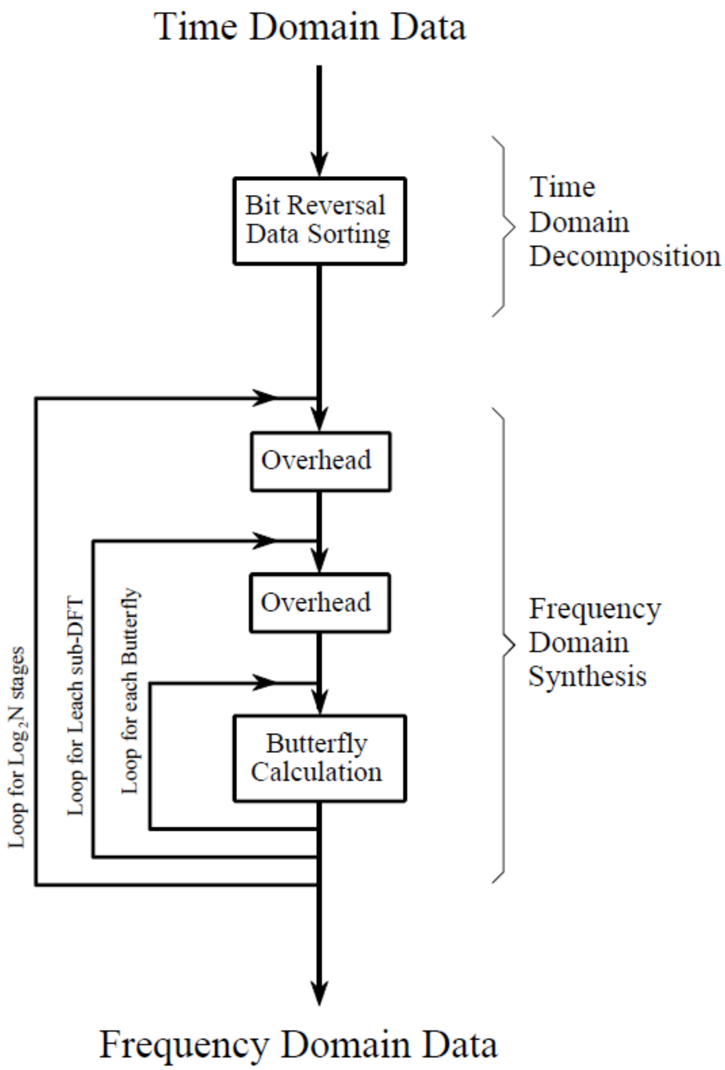

Figure 20. Flow Diagram of the FFT

This is based on three steps: (1) decompose an *N* point time domain signal into *N* signals each containing a single point, (2) find the spectrum of each of the *N* point signals (nothing required), and (3) synthesize the *N* frequency spectra into a single frequency spectrum. The overhead boxes determine the beginning and ending indexes for the loops.
Source: http://www.dspguide.com/ch12/2.htm

Let us consider the computation of the $N = 2^v$ ($N = 512$ and $v = 9$ are the numbers used in this project) point DFT by the Decimation-in-time decomposition. We split the N point data sequence into two $N/2$ point data sequences $f_1(n)$ and $f_2(n)$, corresponding to the even-numbered and odd-numbered samples of $x(n)$, respectively:

$$\begin{aligned} f_1(n) &= x(2n) \\ f_2(n) &= x(2n+1), \qquad n = 0, 1, \cdots, {}^{N}\!/_{2} - 1 \end{aligned}$$

(7)

Thus $f_1(n)$ and $f_2(n)$ are obtained by decimating $x(n)$ by a factor of 2, and hence the resulting FFT algorithm is called a decimation-in-time algorithm. Now the N point DFT can be expressed in terms of the DFT's of the decimated sequences as follows:

$$\begin{aligned} X(k) &= \sum_{n=0}^{N-1}\left(x(n)e^{-j\frac{2\pi nk}{N}}\right) \\ &= \sum_{n=0}^{\frac{N}{2}-1}\left(x(2n)e^{-j\frac{2\pi(2n)k}{N}}\right) + \sum_{n=0}^{\frac{N}{2}-1}\left(x(2n+1)e^{-j\frac{2\pi(2n+1)k}{N}}\right) \\ &= \sum_{n=0}^{\frac{N}{2}-1}\left(x(2n)e^{-j\frac{2\pi nk}{\frac{N}{2}}}\right) + \left(e^{-j\frac{2\pi k}{N}}\right) + \sum_{n=0}^{\frac{N}{2}-1}\left(x(2n+1)e^{-j\frac{2\pi nk}{\frac{N}{2}}}\right) \\ &= \mathbf{DFT}_{\frac{N}{2}}\{x(0), x(2), \cdots, x(N-2)\} + W_N^k \cdot \mathbf{DFT}_{\frac{N}{2}}\{x(1), x(3), \cdots, x(N-1)\} \end{aligned}$$

(8)

The mathematical simplifications in (8) reveal that all DFT frequency outputs $X(k)$ can be computed as the sum of the outputs of two length $N/2$ DFTs, of the even-indexed and odd-indexed discrete-time samples, where the odd-indexed short DFT is multiplied by twiddle factor (W_N^k) term. This reorganization and reuse has reduced the total computation by almost a factor of two over direct DFT computation.

iii. Powered Wheelchair Interface

The printed circuit board (PCB) in figure 21 was designed and fabricated to interface the controller with the powered wheelchair. This PCB houses two dsPIC30F microcontrollers dedicated for speech recognition and FFT analysis. The dsPIC performing the speech recognition is connected to the Si3000 voice CODEC for sampling the input voice from its MIC input. Other dsPIC performing FFT on the accelerometer data is directly connected to the speech recognition dsPIC via 8 digital inputs (for detected voice commands) and is also capable of reading other sensory inputs such as distance sensors. A digital-to-analog converter is used to connect this controller to the joystick of the powered wheelchair. The direction commands from the joystick to the wheelchair's unit are controlled over 2 analog inputs. These inputs are bypassed from the joystick with the inputs from our controller. Out of these two wires one is used to control the movement in forward/backward direction and the other is used to control the right/left direction of movement. To keep the chair in the neutral mode both of these wires must be at +2.5 V. Voltage above this threshold will result in forward/right movement and the voltage below this threshold results in backward/left movement. Deviation of ±1.5 V is allowed on these lines and the speed of the movement is proportional to the amount of voltage deviation from +2.5 V.

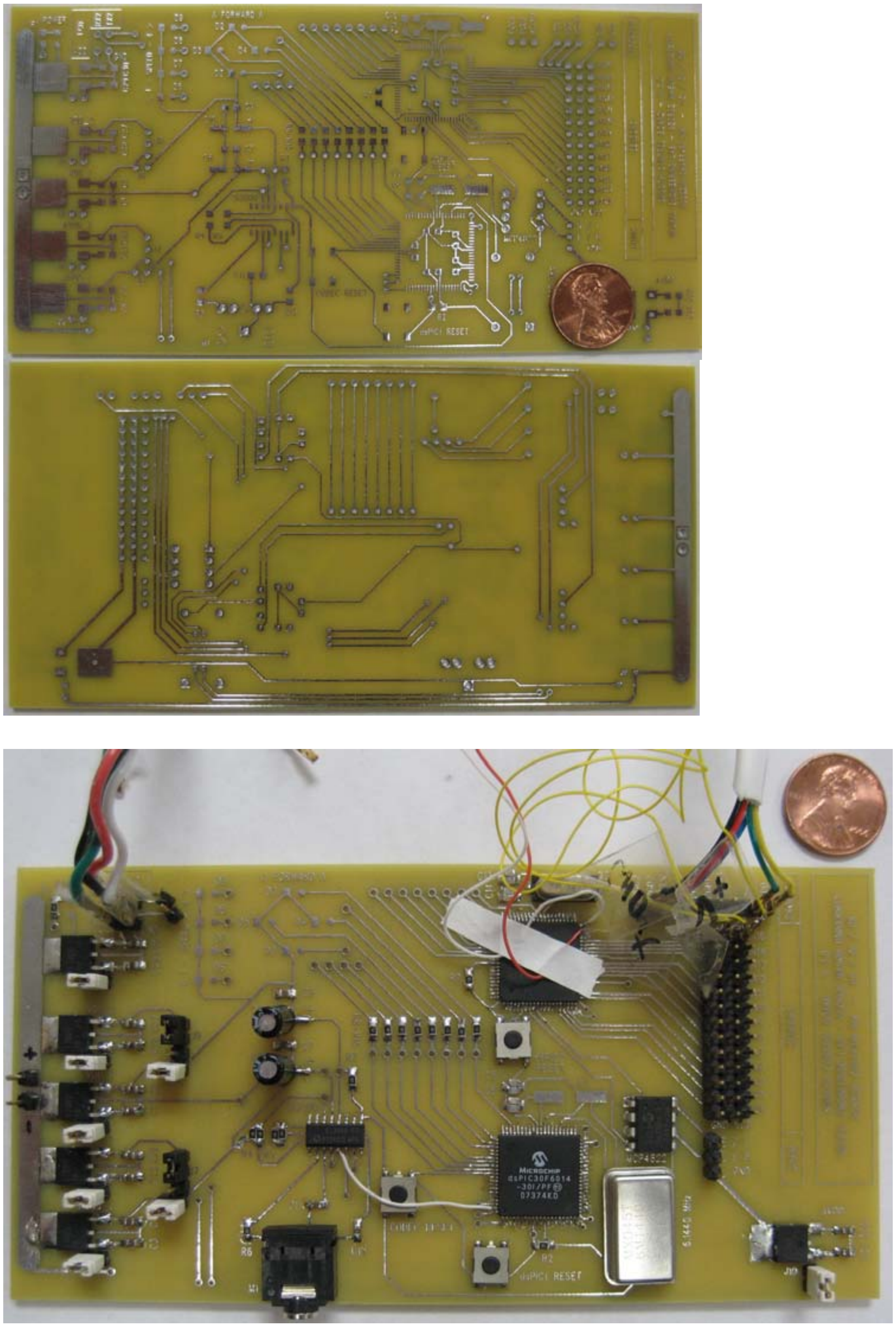

Figure 21. Hum-Power Controller Board

The dimensions of the Hum-power board are 3x6 inches.

Figure 22 shows the block diagram of the current Hum-Power prototype. The touch screen display is currently used only as user interface and is not used to collect input from the user. This controller runs on the 15 V power coming to the chair's joystick and is turned on as soon as the chair is turned on using the joystick. Then the controller runs an initial self test for the speech recognition and requests the user to speak a keyword.

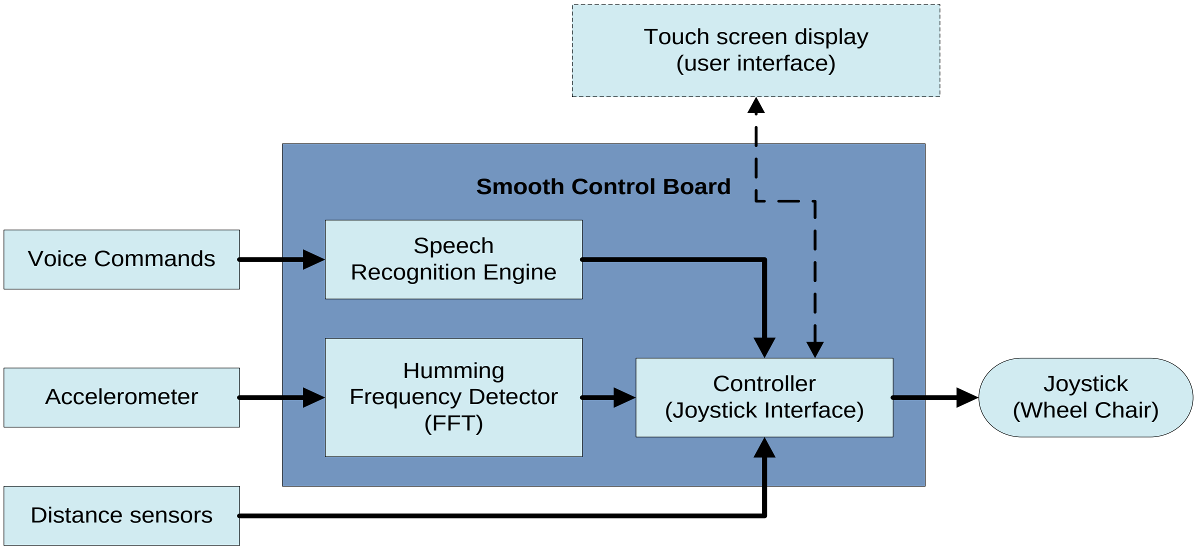

Figure 22. Block Diagram of the Hum-Power Controller

The Hum-Power board is consisted of three major modules. Speech recognition engine which is included in one of the dsPIC's on the board and humming frequency detection and FFT performed on a separate dsPIC which is connected to the joystick controller interface and the touch screen display for user interface. This board is powered via the joystick's 15 V power and controls the joystick via 2 wires for back/forward and right/left.

Figures 23-25 show the schematics used for prototyping the Hum-power controller. There are three main components in the design of this controller: dsPIC1 dedicated for speech recognition, dsPIC2 for performing FFT and communication with the powered wheelchair and the CODEC for sampling the spoken commands to be recognized.

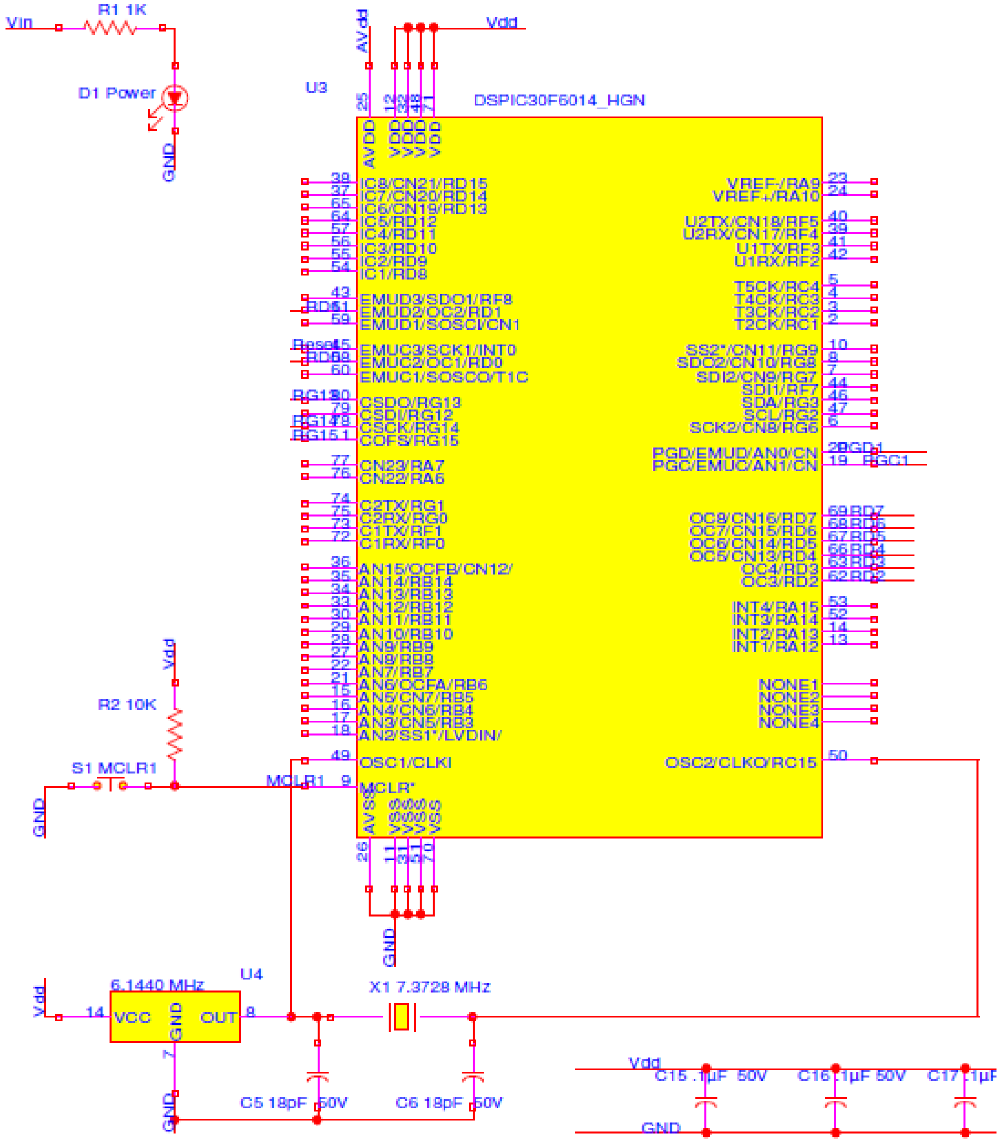

Figure 23. Schematics of dsPIC for Speech Recognition

Using dsPIC30F6014 to perform speech recognition on the sampled voice from the CODEC (Fig. 25). This dsPIC runs independent of the other dsPIC for FFT (Fig. 24) but outputs data through 8 digital ports to other dsPIC.

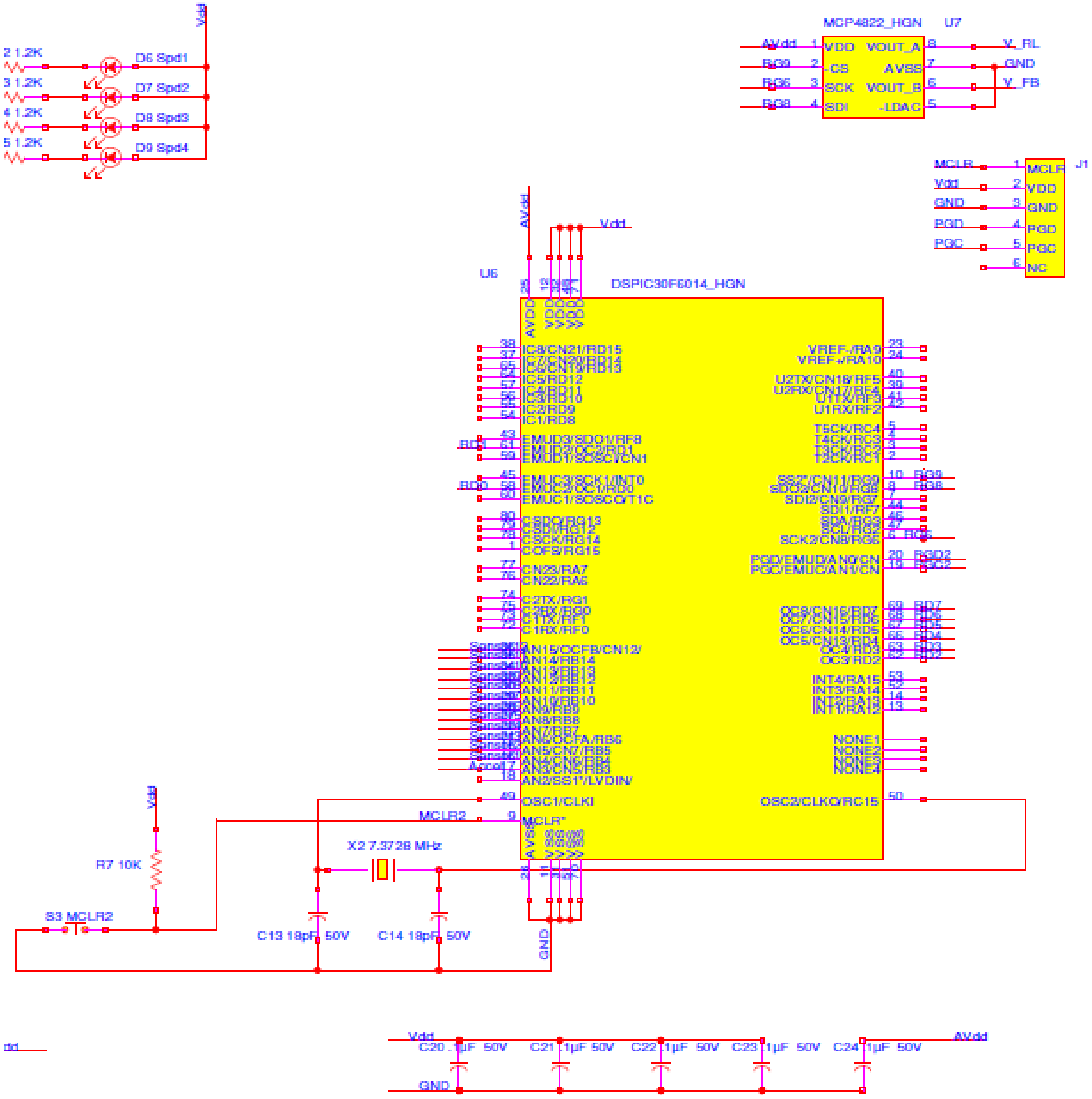

Figure 24. Schematics of dsPIC Performing FFT

Using dsPIC30F6014A the commands recognized by the speech recognition dsPIC (Fig. 23) are captured and analyzed. The control commands are then sent to a dual digital-to-analog converter to perform movement control of the powered wheelchair.

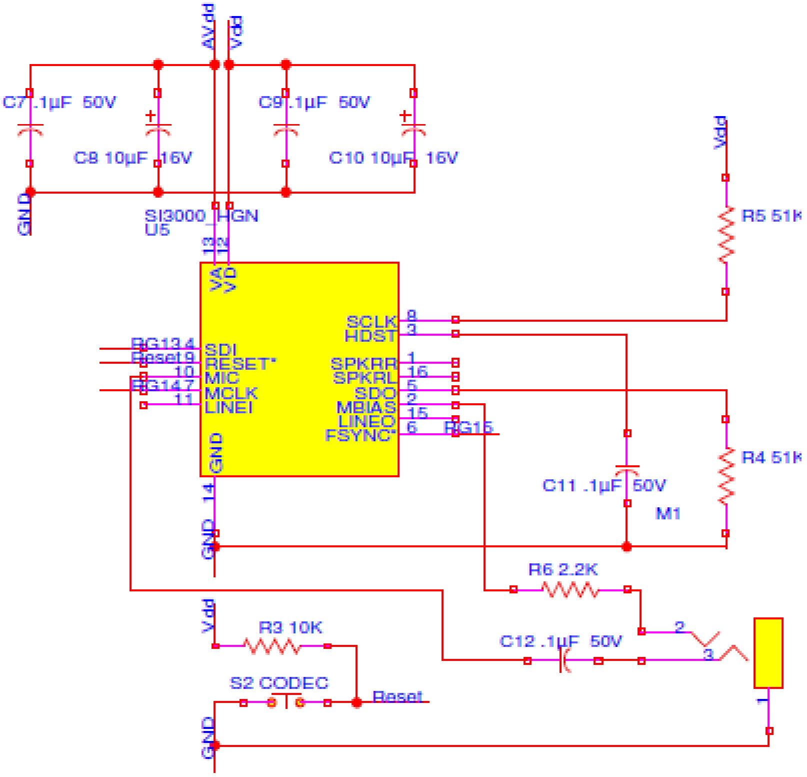

Figure 25. Schematics of Si3000 CODEC

Using Si3000 CODEC the spoken commands are sampled and transferred to the speech recognition dsPIC (Fig. 23). The 3.5 mm microphone jack is connected to this chipset.

3.4. Ambient Noise Test Results

The analysis for the ambient noise effect on the recognition accuracy of the Hum-power controller was done with MATLAB on the “stop” command. The user was asked to repeat this word for 20 times and a 4 second wave-file was recorded for each instant. The same recordings were played back using a computer to be measured and analyzed on a different computer during all the noise tests for better analysis of the data. The power of these signals in the presence of no added white Gaussian noise was calculated and is plotted in figure 26.

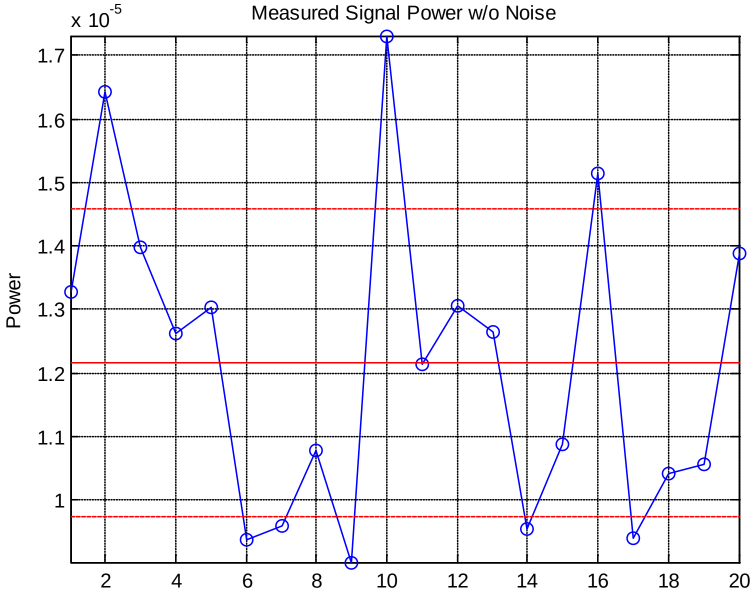

Figure 26. Measured Signal Power without added Noise

The word "stop" was recorded 20 times for 4 seconds in each instance. The recorded signals were in the presence of usually ambient noise without any added Gaussian white noise. The power of these signals was calculated using MATLAB. This shows that different recordings of command "stop" had different power levels given that the ambient noise was not constant at all time and that the user pronounced the word differently at different instances.

To simulate higher ambient noise a white Gaussian noise source was used (2 feet away from the microphone) to increase the noise in the background while recording the commands for analysis. The first recorded "stop" command was then played back for 20 times and at each instance the level of white Gaussian noise was increased by 5% from 0 to a full 100%. Figure 27 shows the calculated power for the measured signal with the presence of added noise. It was observed that with the increase of the noise level the power of the measured signal increased.

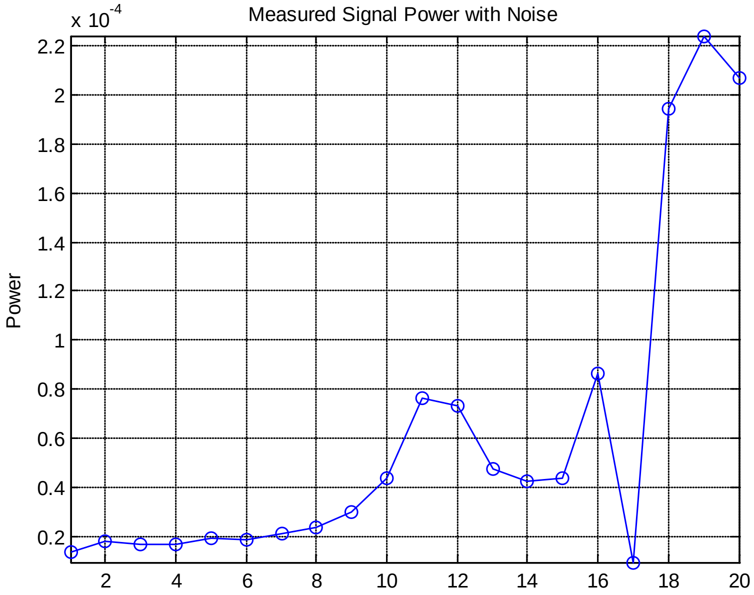

Figure 27. Measured Signal Power at Different White Gaussian Noise Levels

The same recorded “stop” command was played back 20 times and the noise level was increased from 0 to 100% for each instance. It was observed that the power of the measured signal increased with the increase of noise level.

By subtracting the known signal power from the measured noisy signal the actual noise power was calculated. Figure 28 shows the calculated noise power from the measured noisy signal.

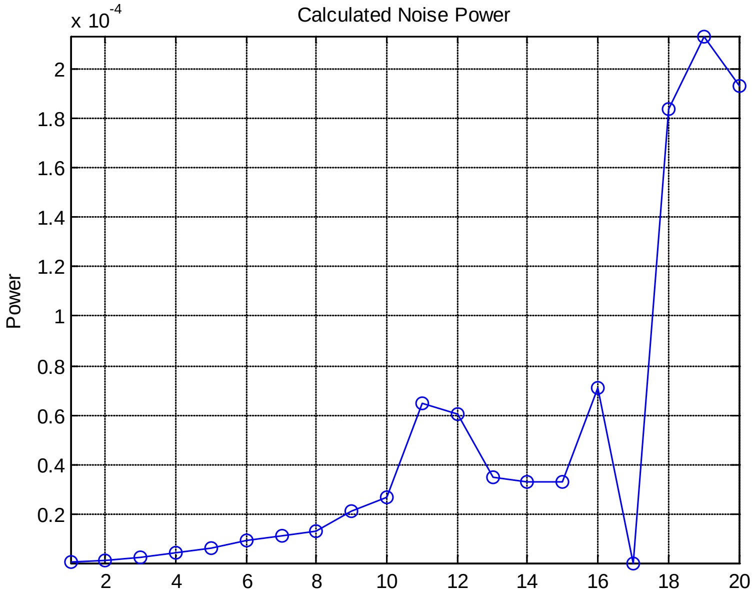

Figure 28. Calculated Noise Power from the Measured Noisy Signal

---

The power of Gaussian noise was calculated using the known signal power and the power of the measured noisy signal. This shows that the power of the Gaussian noise was increasing as expected.

The signal-to-noise ratio (SNR) of the measured signals was then calculated using the following equation. Figure 29 shows that the SNR decreases as the level of added noise increases.

$$SNR = 10\log_{10}\left(\frac{signal\ power}{noise\ power}\right) \quad \textbf{(9)}$$

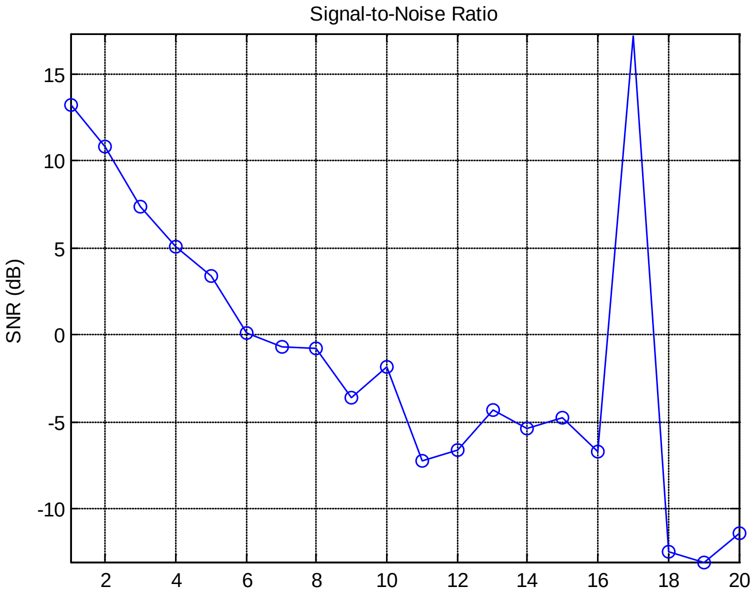

Figure 29. Calculated Signal-to-Noise Ratio of the Measured Noisy Signal

The SNR of the measured signal was calculated using the known signal power and the calculated noise power. The SNR decreases as the noise level increases. Higher SNR are desired for better speech recognition accuracy.

For a more accurate analysis the noise power was calculated for each intensity level. Using the later method the noise power was calculated 20 times for each intensity using the same sample recording. Figure 30 shows that the noise power increases as the intensity of the noise in increased. Using the results of this test the profile of noise power was created for the given white Gaussian noise source at different levels. It was observed that the noise power begins to plateau after intensity level of 55% so the intensity levels of 0 to 50% were used for testing of speech recognition accuracy.

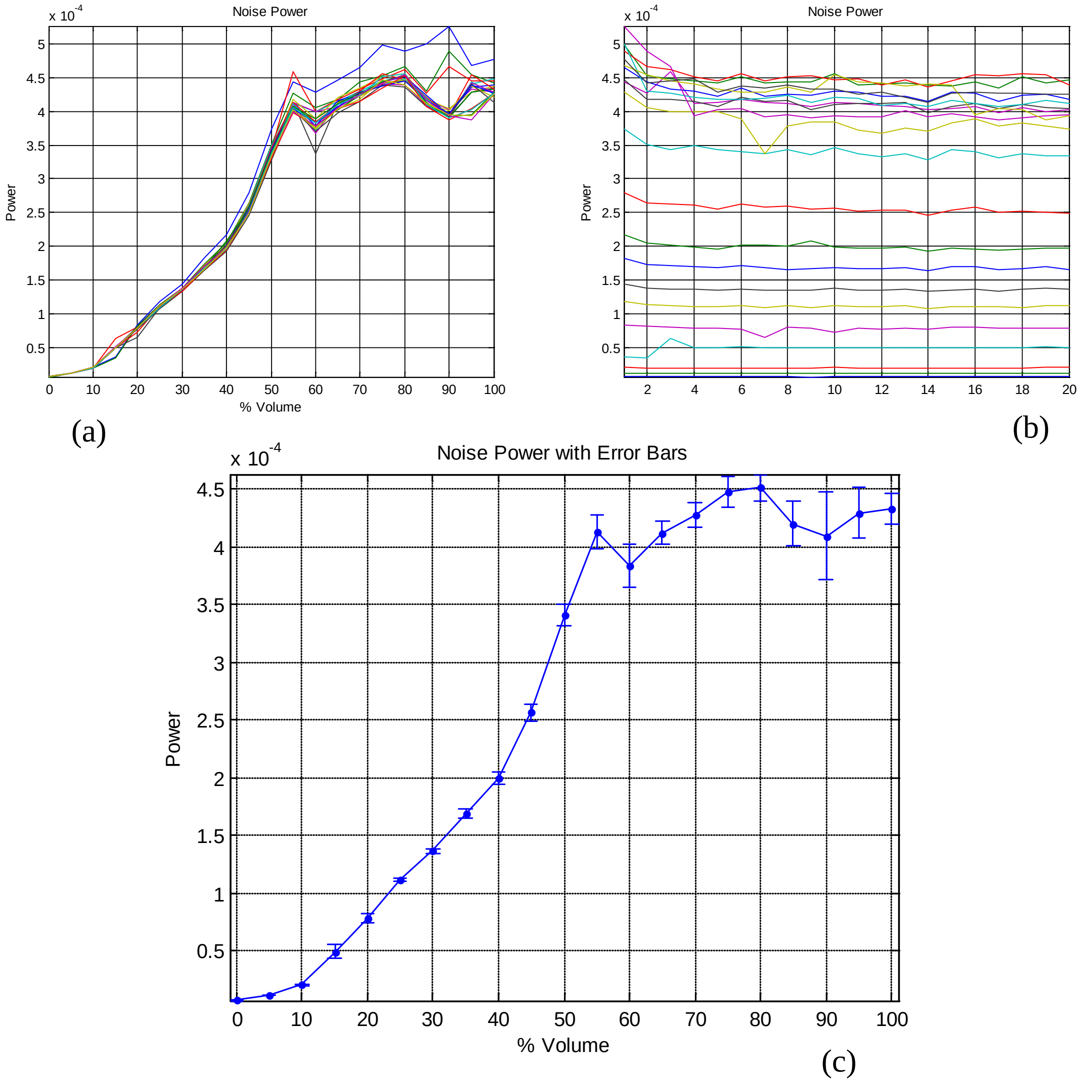

Figure 30. Power Profile for the Noise Source at Different Intensity Levels

---

(a) Shows 20 traces of noise power measurements for different intensity levels. This plot shows that the power at all instances increased as the intensity level of the noise was increased. (b) Shows the change in the power level for each intensity during the 20 instances. This plot shows that the noise power was relatively constant for 20 instances for a given intensity level. (c) Shows the average and deviation of the noise power for each intensity level. This plot shows that the measured noise power is accurate and reliable for the intensity levels of less than 50%. Large deviation in the higher intensities prevented us from using them in our test for accuracy.

The same 20 recordings of the word “stop” where used for the test of accuracy in speech recognition. To test the reliability of the measured signal powers (without added noise) the recordings were played back 5 times and their signal power was measured for each instance. Figure 31 shows the reliability of signal power measurement for the spoken commands.

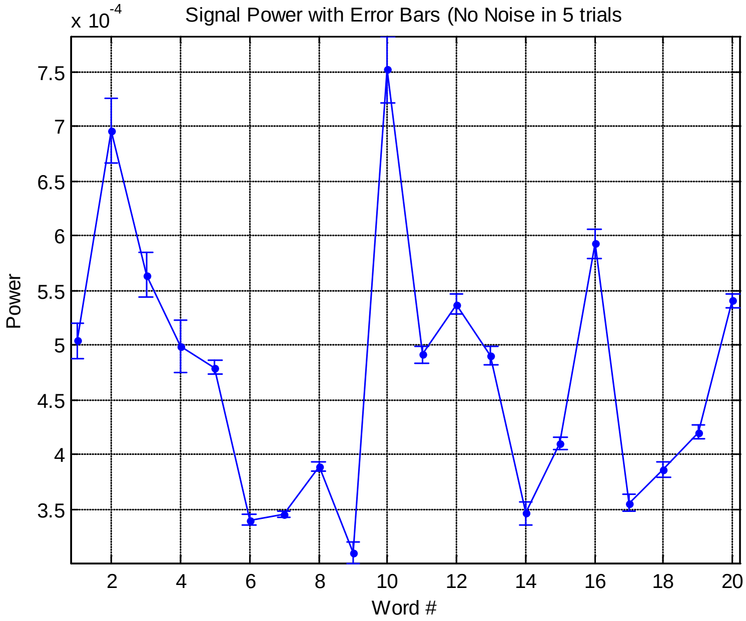

Figure 31. Reliability of Signal Power Measurement for the Spoken Words

The set of 20 “stop” words recorded was played back 5 times without any added noise and for each instance the signal power was measured. This plot shows that the measurement of the signal power is reliable and accurate.

To test for the accuracy of recognition the set of 20 “stop” commands was played back and recognized by the Hum-power controller in 6 different noise intensity levels. Using the noise power profile of figure 30 and the signal power measurement in figure 31 the SNR of recognized words was calculated. Figure 32 shows the SNR of each recognized word at different noise intensity levels with the percent accuracy of the speech recognition at different SNR levels.

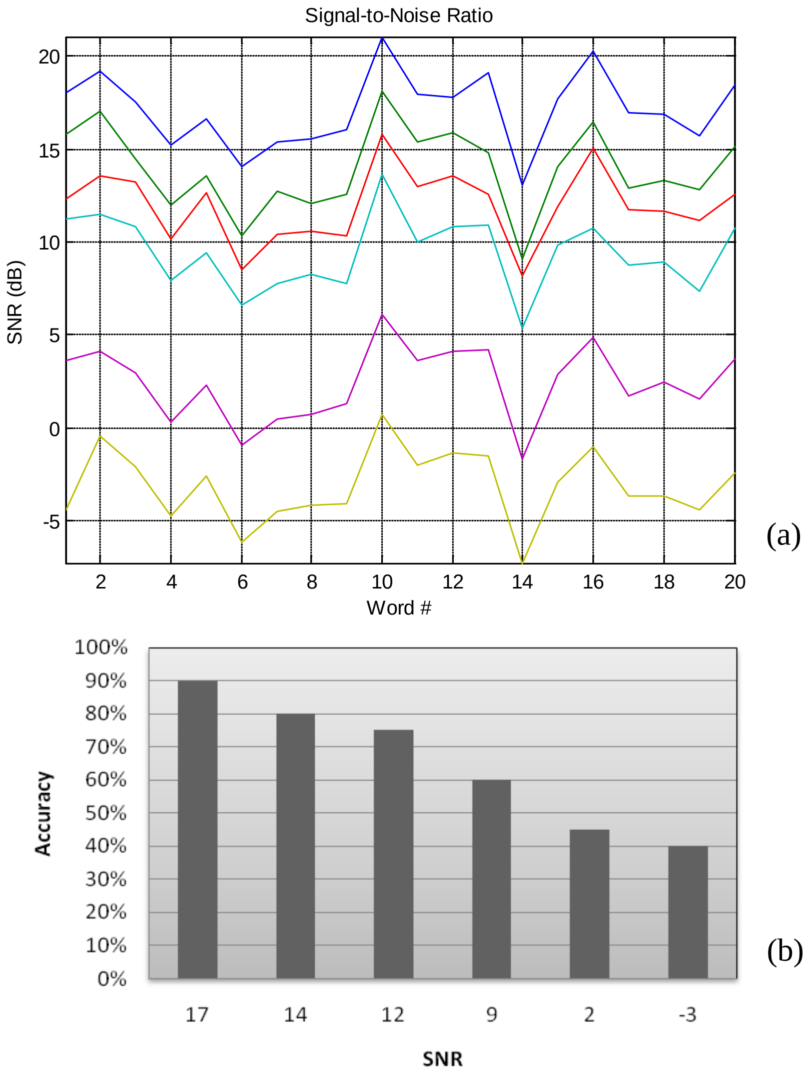

Figure 32. Speech Recognition Accuracy at Different SNR Levels

(a) Shows the SNR of the tested commands for 6 different noise levels. (b) Shows the present accuracy of the speech recognition for an average SNR level recorded.

3.5. Field Test Results

The final prototype of the Hum-power controller was presented and demonstrated to the public during the Engineering Day at George Mason University. This demonstration was to test the functionality and reliability of this product in real life situation such as busy and crowded environments. The Hum-powered controller was put to test by visitors of male and female of all ages. Due to the speaker independence speech recognition technology of the Hum-power no voice training was required for different users. The concept of control was easy to understand for all the testers and all the users were able to perform smooth maneuvering using voice commands mixed with humming. Speech recognition in the presented high ambient noise proved to be about 70% accurate for female and about 80% accurate for the male users. All users except one female tester were able to perform smooth movement with variable speed using humming.

In general the Hum-power controller was tested to be usable by all testers with a brief introduction to the control concept. Speech recognition accuracy was the only shortcoming that was observed during the entire test. The first prototype of the Hum-power controller tested provided evidence that the concept of the control technique is promising and adequate and revealed the need for better speech recognition engine.

Chapter 4: Discussion

4.1. What Was Achieved in This Thesis

In this thesis a new and innovative controller interface for powered wheelchairs was investigated, proposed, and designed. The prototype of the Hum-Power controller was implemented and successfully tested on the Invacare's Storm TDX5 (mid-wheel drive power chair) donated to us by East Coast Rehab, LLC. Hum-Power controller enables its users to control their powered wheelchairs via voice commands and provides them with accurate and smooth control over the speed if needed using humming. This controller is capable of translating the user's frequency of the humming to their desired speed of movement for maneuvering in environments that required precise control. This controller can be easily interfaced with the joystick available on the user's current wheelchair. The ambient noise testing for speech recognition proves near 90% accuracy in signal to noise ratio (SNR) of about 15dB. This working product of Hum-Power controller showed that such controllers with speech and hum recognition are possible to be implemented and marketed as successful and innovative new powered wheelchair controller.

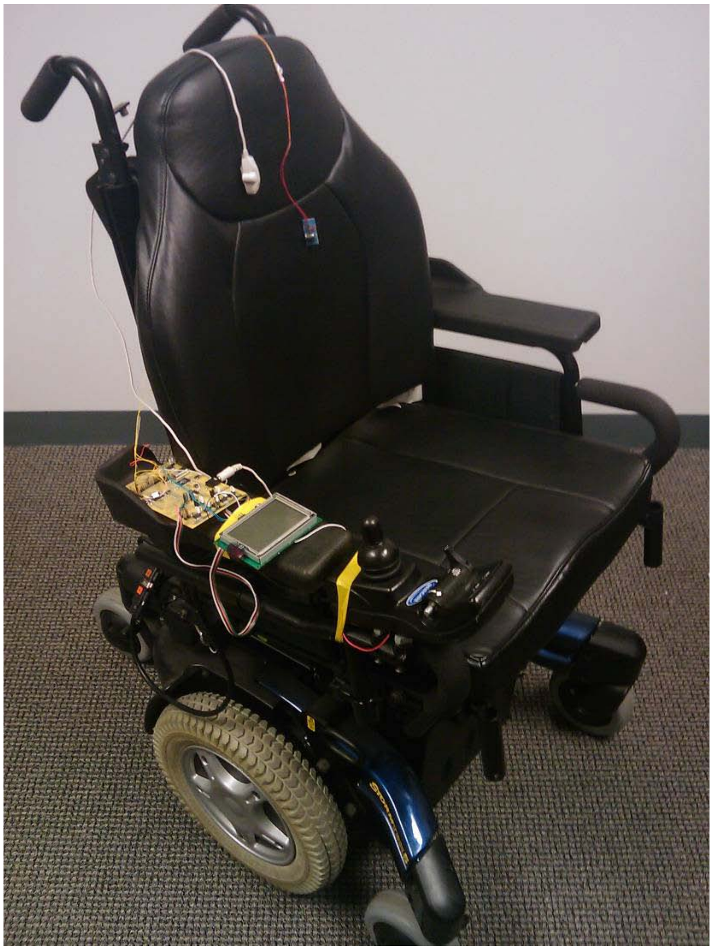

Figure 33. Hum-power Controller Installed on Powered Wheelchair

---

This is the Hum-power controller installed on our test powered wheelchair. The Hum-power controller board is visible on the hand-rest of the chair (on the left) and is connected to the display (middle) and the chair's joystick (right). The Hum-power board is powered through the battery of the chair and is cable of speech recognition for voice command and humming detection for smooth speed control of the movement.

The main problems we encountered were the lack of detailed specification and schematics on the commercially available joysticks and powered wheelchair main control units. Due to the lack of this information we were not able to hack into the main control unit of the powered wheelchair to better interact with the controller or to receive feedback from the chair while in operation. To solve this problem we traced and reverse engineered the joystick to find and understand the main control lines for the powered wheelchair.

Finding a suitable speech recognition solution for this project also presented some issues. The original speech recognition chipset HM2007 selected was tested to have close to 70% accuracy on the speaker dependence base recognition and required the commands to be recorded and stored before use. As the result of these shortcomings this solution was abandoned and dsPIC30F microcontroller was selected for faster and more accurate speaker independent speech recognition. We also discovered that since a continuous speech recognition was required during the operation of the chair two different dsPICs needed to be implemented for the Hum-power controller. Given that the speech recognition and FFT are both complicated processes we designed the controller to have a separate dsPIC for each of these operations.

4.2. Future Work

The Hum-power controller presented in this thesis project proved to be promising and for future commercialization of this product a number of improvements are required. For truly autonomous control of the today's powered wheelchair it is important to develop an indoor/outdoor guidance system with obstacle avoidance capabilities. The original prototype developed in this thesis project is capable of handling analog inputs from distance sensors such as sonar and infrared proximity sensors. By taking advantage of these sensory inputs in the final product the Hum-power controller would be able to handle obstacle in its rout. With the immerging technologies for indoor positioning such as Ekahau Positioning Engine ™ (EPE) WiFi based system the Hum-power controller could be linked to smart homes with positioning capabilities so that minimal effort would be required for the user to navigate to a desired point in the house.

An improved version of the Hum-power controller could be redesigned to be implemented on Pocket PCs and PDAs (personal digital assistant), given that today's available PDAs are all equipped with wireless communication peripherals such as Bluetooth and WiFi with GPS (global positioning system) chipsets built-in. Other improvements can be done such as adding smart distance sensing management so that if the chair is maneuvering through a small opening it could overwrite and correct the given commands. It is also possible to introduce joystick overwrite capability to the controller. By adding switches to the controller or implementing input-change detectors in the microcontroller it is possible to enable outside control of the powered wheelchair to a nurse. Using a better speech recognition engines such as the ones used in today's cell phones and PDAs the Hum-power controller could recognize a larger vocabulary of commands (even supporting different languages) faster and more accurate for a more dependable final product.

APPENDIX

Operation Manual

Hum-power controller is installed with your regular joystick and bypasses the connection from the joystick to the powered wheelchair in order to operate the wheelchair through your voice commands. For using the Hum-power controller you need wear the microphone/accelerometer unit on your neck. The microphone needs to be adjusted within 2 inches of your mouth and the accelerometer needs to be placed on the neck as illustrated in this picture:

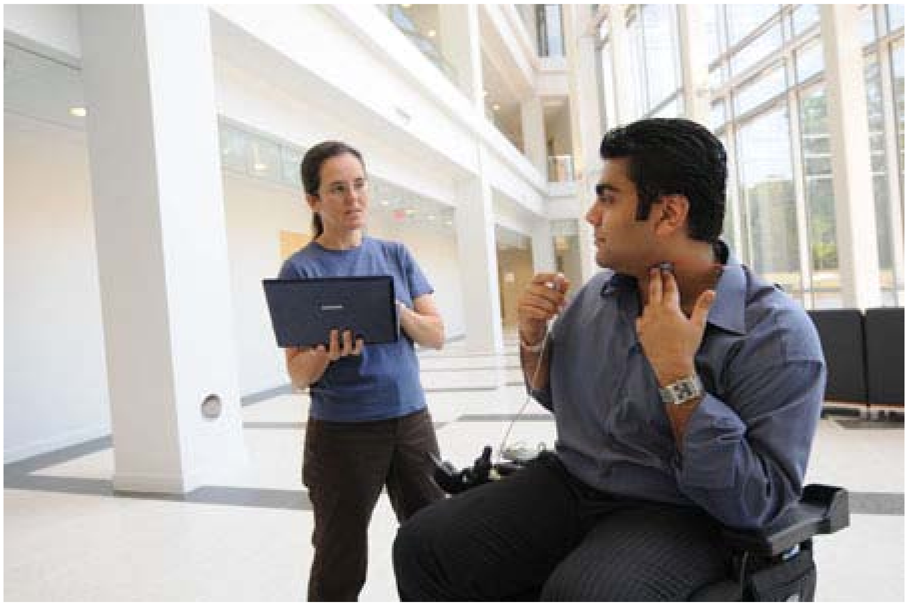

Hum-power controller is designed to be powered from your wheelchair battery and it is operational when the wheelchair is turned on. Hum-power controller is equipped with a display which is used to help the users with available voice commands at each given time. Hum-power controller performs a self test of the system at each initial startup to insure the operation of the device. If the system is ready to be used the following screen is presented to the user:

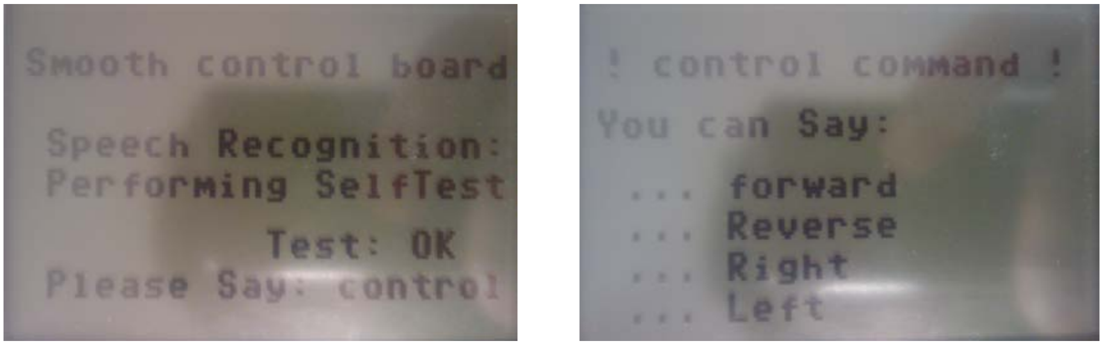

```
Smooth control board

 Speech Recognition:
 Performing SelfTest

           Test: OK
 Please Say: control
```

```
! control command !
You can Say:
 ... forward
 ... Reverse
 ... Right
 ... Left
```

Figure A-1: Initial Self Test & "Control" Command Display

When the "Control" command is given by the user the system activates the humming control mode of the interface and a second help menu is displayed. In this mode the user is asked for the direction of the movement desired (i.e. right, left, forward or reverse). After the direction command is given the available commands for this mode are all given to the system and the resulted movement description is shown on the display. The user is required to hum to control the speed of the movement in this mode. Higher frequency of humming results in higher speed of movement in a linear form.

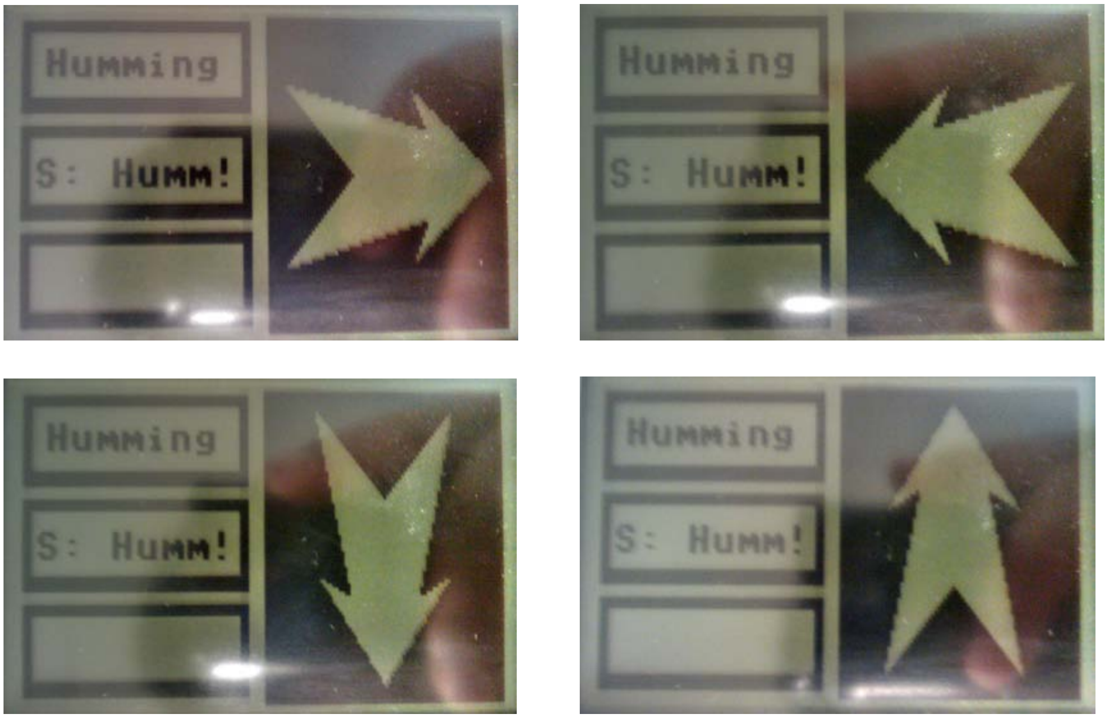

Figure A-2: Direction in Manual Mode Display

At any point if the given command is not recognized the following screen is displayed to get the user started with a desired mode of operation:

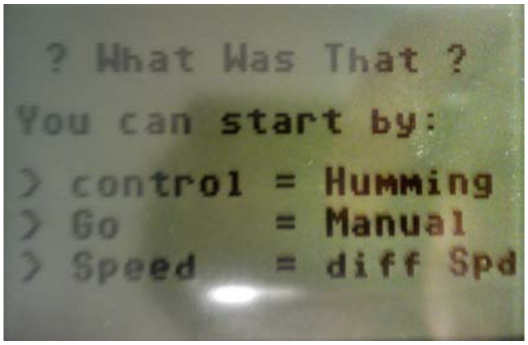

```
 ? What Was That ?
You can start by:
> control  = Humming
> Go       = Manual
> Speed    = diff Spd
```

Figure A-3: Error in Speech Recognition Display

Users can perform maneuvers in the manual mode by giving the “Go” command. This mode is similar to the humming mode, but after the direction command is given speed is set to be at level of 25%.

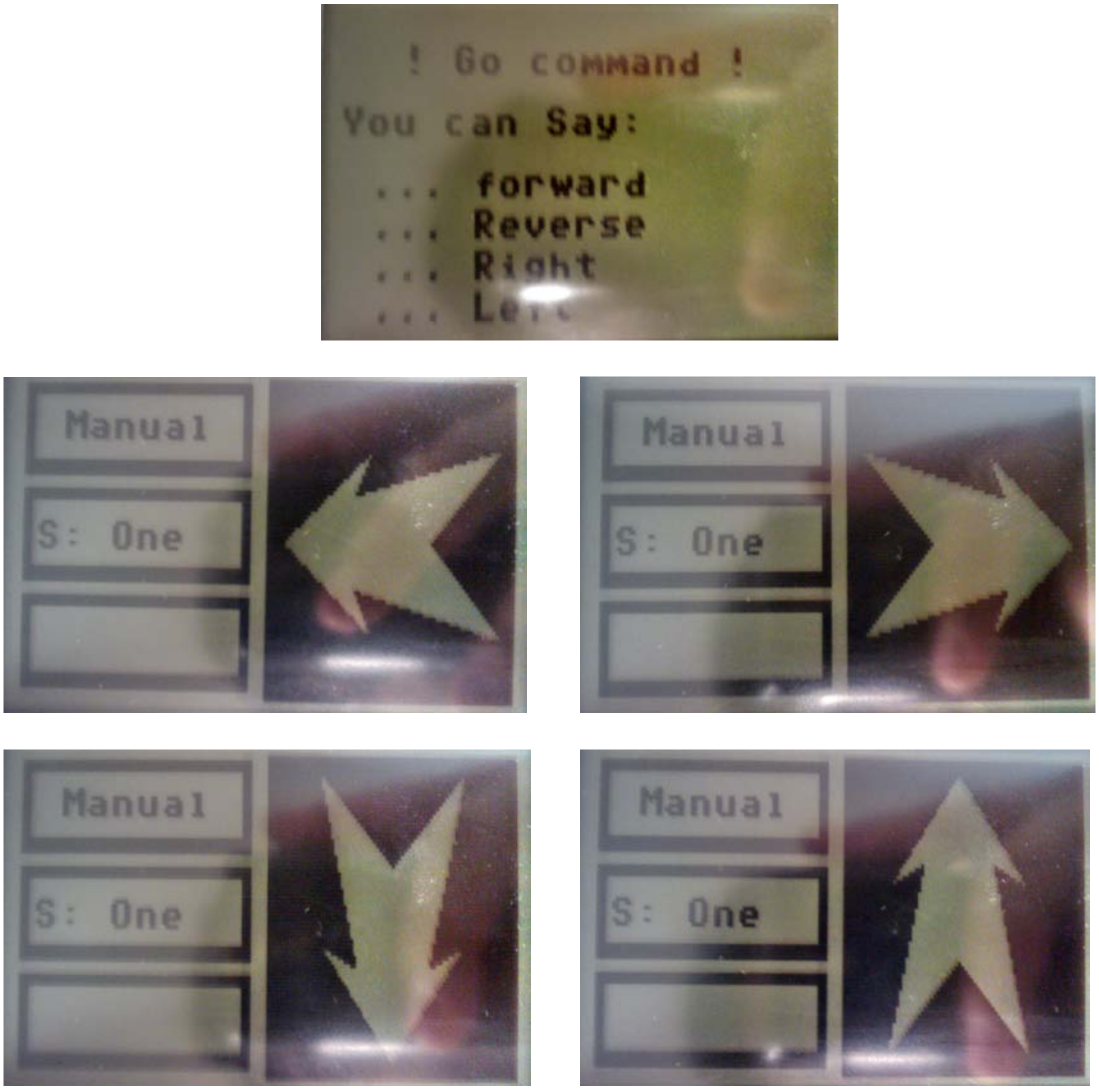

Figure A-4: “Go” Command and Direction in Automatic Mode Display

While in manual mode the initial speed of one can be changed using the “Speed” command. This command only works with the manual mode and with four speed levels of one, 25%, two, 50%, three, 75% and four with 100% of the available speed the user is able to increase or decrease the speed of movement. By giving the “Speed” command the following screens are displayed:

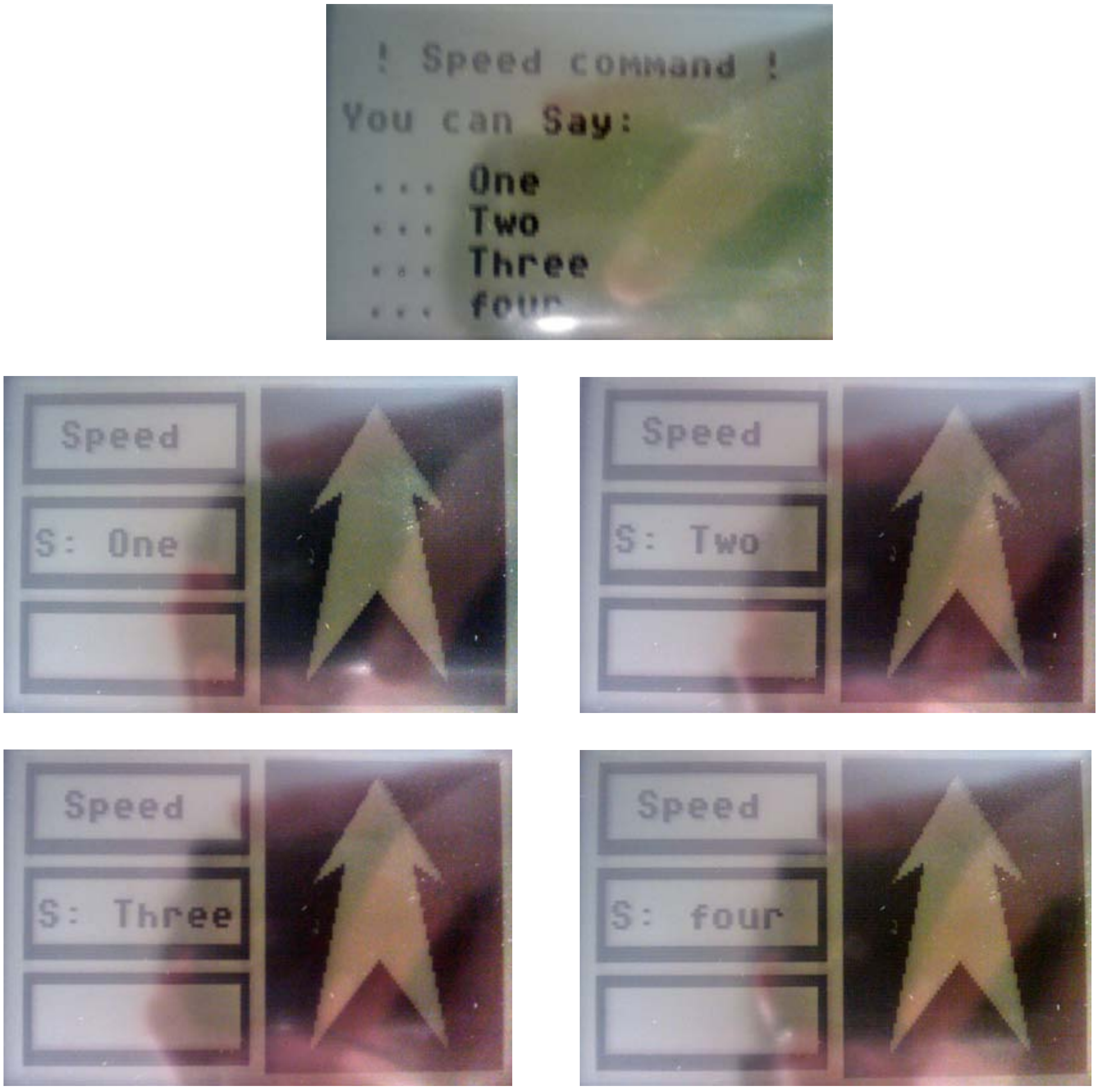
! Speed command !
You can Say:
... One
... Two
... Three
... four

Figure A-5: “Speed” Command and Different Speed in Automatic Mode Display

REFERENCES

REFERENCES

[1] S. Aoshima, H. Kaminaga and M. Shiraishi, "One-hand drive-type power-assisted wheelchair with a direction control device using pneumatic pressure," *Adv. Rob.,* vol. 16, pp. 773-84, 2002.

[2] K. Arshak, D. Buckley. Review of Assistive Devices for Electric Powered Wheelchairs Navigation. ITB Journal, vol. 13, pp. 13-23, 2006

[3] D. Bayer, J. Springsteen and R. Nash, "A next generation intelligent wheelchair control system," in *Technology and Persons with Disabilities,* 1992, pp. 41-5.

[4] M. Brookes, "VOICEBOX, the Speech Processing Toolbox for MATLAB," v 1.5, London, 2006.

[5] Chung-Hsien Kuo and H. H. W. Chen, "Human-Oriented Design of Autonomous Navigation Assisted Robotic Wheelchair for Indoor Environments," *Mechatronics, 2006 IEEE International Conference on,* pp. 230-235, 2006.

[6] Chung-Hsien Kuo, Hung-Wen Yeh and Chin-En Wu, "Development of autonomous navigation robotic wheelchairs using programmable System-on-Chip based distributed computing architecture," *Systems, Man and Cybernetics, 2007. ISIC. IEEE International Conference on,* pp. 2939-2944, 2007.

[7] Chung-Hsien Kuo, Hung-Wen Yeh, Chin-En Wu and Ko-Ming Hsiao, "Development of Autonomous Robotic Wheelchair Controller Using Embedded Systems," *Industrial Electronics Society, 2007. IECON 2007. 33rd Annual Conference of the IEEE,* pp. 3001-3006, 2007.

[8] Chung-Hsien Kuo, Jia-Wun Siao and Kuo-Wei Chiu, "Development of an intelligent power assisted wheelchair using fuzzy control systems," *Systems, Man and Cybernetics, 2008. SMC 2008. IEEE International Conference on,* pp. 2578-2583, 2008.

[9] R. A. Cooper, "Intelligent control of power wheelchairs," *Engineering in Medicine and Biology Magazine, IEEE,* vol. 14, pp. 423-431, 1995.

[10] R. A. Cooper, M. L. Boninger, D. M. Spaeth, D. Ding, Songfeng Guo, A. M. Koontz, S. G. Fitzgerald, R. Cooper, A. Kelleher and D. M. Collins, "Engineering

Better Wheelchairs to Enhance Community Participation," *Neural Systems and Rehabilitation Engineering, IEEE Transactions on,* vol. 14, pp. 438-455, 2006.

[11] D. Ding and R. A. Cooper, "Electric powered wheelchairs," *Control Systems Magazine, IEEE,* vol. 25, pp. 22-34, 2005.

[12] N. R. Dixon and T. B. Martin, *Automatic Speech & Speaker Recognition.* New York: IEEE Press : distributor, Wiley, 1979, pp. 433.

[13] P. M. Faria, R. A. M. Braga, E. Valgode and L. P. Reis, "Interface Framework to Drive an Intelligent Wheelchair Using Facial Expressions," *Industrial Electronics, 2007. ISIE 2007. IEEE International Symposium on,* pp. 1791-1796, 2007.

[14] A. Fattouh and S. Nader, "Preliminary Results on Dynamic Obstacle Avoidance for Powered Wheelchair," *Information and Communication Technologies, 2006. ICTTA '06. 2nd,* vol. 1, pp. 849-853, 2006.

[15] L. Fehr, W. E. Langbein and S. B. Skaar, Adequacy of power wheelchair control interfaces for persons with severe disabilities: A clinical survey, *Journal of Rehabilitation Research and Development*. vol. *37* no. 3, 2000, pp. 353-360.

[16] T. Felzer and B. Freisleben, "HaWCoS: The "hands-free" wheelchair control system," in *ASSETS 2002: Proceedings of the 5th International ACM SIGCAPH Conference on Assistive Technologies, July 08,2002 - July 10,* 2002, pp. 127-134.

[17] M. Fezari and A. -. Khati, "New speech processor and ultrasonic sensors based embedded system to improve the control of a motorised wheelchair," *Design and Test Workshop, 2008. IDT 2008. 3rd International,* pp. 345-349, 2008.

[18] J. Hansen, NexTTool. NexTTool is developed by John Hansen and is freely distributed as part of the BrixCC NXT development suite, 2006.

[19] C. S. Harrison, M. Grant and B. A. Conway, "Haptic interfaces for wheelchair navigation in the built environment," *Presence,* vol. 13, pp. 520-34, 10. 2004.

[20] C. Huddleston, *Intelligent Sensor Design using the Microchip dsPIC.* Amsterdam ; Boston: Elsevier/Newnes, 2007, pp. 283.

[21] T. Joseph and Hung Nguyen, "Neural network control of wheelchairs using telemetric head movement," *Engineering in Medicine and Biology Society, 1998. Proceedings of the 20th Annual International Conference of the IEEE,* vol. 5, pp. 2731-2733 vol.5, 1998.

[22] K. Kuah, M. Bodruzzaman and S. Zein-Sabatto, "A neural network-based text independent voice recognition system," *Southeastcon '94. 'Creative Technology Transfer - A Global Affair'. , Proceedings of the 1994 IEEE,* pp. 131-135, 1994.

[23] Y. Kuno, N. Shimada and Y. Shirai, "Look where you're going [robotic wheelchair]," *Robotics & Automation Magazine, IEEE,* vol. 10, pp. 26-34, 2003.

[24] W. N. Lam, A. F. T. Mak, W. C. Tam and R. A. Cooper, "Kinematics of the wrist, elbow and shoulder during manual wheelchair maneuvers," *[Engineering in Medicine and Biology, 2002. 24th Annual Conference and the Annual Fall Meeting of the Biomedical Engineering Society] EMBS/BMES Conference, 2002. Proceedings of the Second Joint,* vol. 3, pp. 2573-2576 vol.3, 2002.

[25] S. P. Levine, D. A. Bell, L. A. Jaros, R. C. Simpson, Y. Koren and J. Borenstein, "The NavChair Assistive Wheelchair Navigation System," *Rehabilitation Engineering, IEEE Transactions on,* vol. 7, pp. 443-451, 1999.

[26] Liu Chong and Wang Hong, "The Design of Wheelchair Based on SEMG Control," *Bioinformatics and Biomedical Engineering, 2008. ICBBE 2008. the 2nd International Conference on,* pp. 1721-1724, 2008.

[27] Y. Matsumotot, T. Ino and T. Ogsawara, "Development of intelligent wheelchair system with face and gaze based interface," *Robot and Human Interactive Communication, 2001. Proceedings. 10th IEEE International Workshop on,* pp. 262-267, 2001.

[28] L. Mclaughlin, "Silencing voice recognition technology," *Intelligent Systems, IEEE,* vol. 19, pp. 4-6, 2004.

[29] S. Molau, M. Pitz, R. Schluter and H. Ney, "Computing Mel-frequency cepstral coefficients on the power spectrum," *Acoustics, Speech, and Signal Processing, 2001. Proceedings. (ICASSP '01). 2001 IEEE International Conference on,* vol. 1, pp. 73-76 vol.1, 2001.

[30] National Spinal Cord Injury Statistical Center, NSCISC Annual Statistical Report - Complete Public Version. 2007. Birmingham, Alabama.

[31] H. G. Nik, G. M. Gutt and N. Peixoto, "Voice Recognition Algorithm for Portable Assistive Devices," *Sensors, 2007 IEEE,* pp. 997-1000, 2007.

[32] S. Oh and Y. Hori, "Development of a novel instantaneous speed observer and its application to the power-assisted wheelchair control," *Power Electronics and Motion Control Conference, 2004. IPEMC 2004. the 4th International,* vol. 3, pp. 1471-1476 Vol.3, 2004.

[33] H. Osada, "Evaluation method for a voice recognition system modeled with discrete Markov chain," *Communications, Computers and Signal Processing, 1997. '10 Years PACRIM 1987-1997 - Networking the Pacific Rim'. 1997 IEEE Pacific Rim Conference on,* vol. 2, pp. 600-602 vol.2, 1997.

[34] G. Pacnik, K. Benkic and B. Brecko, "Voice operated intelligent wheelchair - VOIC," *Industrial Electronics, 2005. ISIE 2005. Proceedings of the IEEE International Symposium on,* vol. 3, pp. 1221-1226 vol. 3, 2005.

[35] A. Papandreou-Suppappola, *Applications in Time-Frequency Signal Processing.* Boca Raton: CRC Press, 2003, pp. 409.

[36] S. P. Parikh, V. Grassi Jr., V. Kumar and J. Okamoto Jr., "Integrating Human Inputs with Autonomous Behaviors on an Intelligent Wheelchair Platform," *Intelligent Systems, IEEE,* vol. 22, pp. 33-41, 2007.

[37] A. M. Peinado, J. C. Segura, A. J. Rubio, P. Garcia and J. L. Perez, "Discriminative codebook design using multiple vector quantization," *Speech and Audio Processing, IEEE Transactions on,* vol. 4, pp. 89-95, 1996.

[38] H. Perez-Meana, *Advances in Audio and Speech Signal Processing : Technologies and Applications.* Hershey, PA: Idea Group Pub., 2007, pp. 446.

[39] Qiang Zeng, B. Rebsamen, E. Burdet and Chee Leong Teo, "A Collaborative Wheelchair System," *Neural Systems and Rehabilitation Engineering, IEEE Transactions on,* vol. 16, pp. 161-170, 2008.

[40] L. R. Rabiner, "A tutorial on hidden Markov models and selected applications in speech recognition," *Proceedings of the IEEE,* vol. 77, pp. 257-286, 1989.

[41] Ruei-Xi Chen, Liang-Gee Chen and Lilin Chen, "System design consideration for digital wheelchair controller," *Industrial Electronics, IEEE Transactions on,* vol. 47, pp. 898-907, 2000.

[42] M. Sajkowski, "Voice control of dual-drive mobile robots-survey of algorithms," *Robot Motion and Control, 2002. RoMoCo '02. Proceedings of the Third International Workshop on,* pp. 387-392, 2002.

[43] J. Sanchez and M. P. Canton, *Microcontroller Programming : The Microchip PIC.* Boca Raton, FL: CRC Press, 2007, pp. 804.

[44] Seung-Hyun Lim and Jae Wook Jeon, "Multiple mobile robot interface using a low cost voice recognition chip," *Robot and Human Communication, 1997. RO-MAN '97. Proceedings. , 6th IEEE International Workshop on,* pp. 402-407, 1997.

[45] R. C. Simpson and S. P. Levine, "Voice control of a powered wheelchair," *Neural Systems and Rehabilitation Engineering, IEEE Transactions on,* vol. 10, pp. 122-125, 2002.

[46] R. C. Simpson and S. P. Levine, "Automatic adaptation in the NavChair Assistive Wheelchair Navigation System," *Rehabilitation Engineering, IEEE Transactions on,* vol. 7, pp. 452-463, 1999.

[47] R. C. Simpson and S. P. Levine, "Adaptive shared control of a smart wheelchair operated by voice control," *Intelligent Robots and Systems, 1997. IROS '97. , Proceedings of the 1997 IEEE/RSJ International Conference on,* vol. 2, pp. 622-626 vol.2, 1997.

[48] R. C. Simpson, D. Poirot and F. Baxter, "The Hephaestus Smart Wheelchair system," *Neural Systems and Rehabilitation Engineering, IEEE Transactions on,* vol. 10, pp. 118-122, 2002.

[49] S. W. Smith, *The Scientist and Engineer's Guide to Digital Signal Processing.* ,1st ed.San Diego, Calif.: California Technical Pub., 1997, pp. 626.

[50] Y. Takahashi, M. Kohda, Y. Shinoda and K. Kubota, "Psychological flutter of robotic wheelchair with inverse pendulum control," *Industrial Electronics, 2008. ISIE 2008. IEEE International Symposium on,* pp. 1318-1323, 2008.

[51] Z. Tan and B. Lindberg, *Automatic Speech Recognition on Mobile Devices and Over Communication Networks.* London: Springer, 2008, pp. 401.

[52] J. Yuan, "Stability analyses of wheelchair robot based on “Human-in-the-Loop” control theory," *Robotics and Biomimetics, 2008. ROBIO 2009. IEEE International Conference on,* pp. 419-424, 2009.

CURRICULUM VITAE

Hossein Ghaffari Nik was born in Tehran, Iran. He moved to the United States in 2001 and graduated from Oakton High School, Fairfax, Virginia, in 2003. Hossein received his Associate of Science in Electrical Engineering from Northern Virginia Community College in 2005. He joined George Mason University in Spring of 2005 and received his Bachelor of Science in Electrical Engineering in 2007. While pursuing his Master of Science he worked as a graduate teaching and research assistant at George Mason University's Electrical and Computer Engineering department.